was used as a secondary Ab. After staining, the hematopoietic cells were analyzed and isolated by flow cytometry on an LSR II and FACSAria flow cytometer, respectively, using FACSDiva software (BD Bioscience).

Colony assay and May-Giemsa staining

The cells (5×10^4 cells) were cultured in a Methocult M3434 medium containing IL-3, IL-6, SCF, and erythropoietin (Stem-Cell Technologies, Inc.) for 10 days. The number of individual colonies was counted by microscopy. The colony number was normalized to the total number of hematopoietic cells. The multipotent hematopoietic progenitor cell-derived colonies (colony-forming unit–granulocyte, erythrocyte, monocyte, megakaryocyte (CFU-GEMM)/CFU-Mix) were picked up, fixed on glass slides using a cytospin centrifuge (Cytospin 4; Thermo Shandon), and stained with May-Grünwald Stain solution (Sigma) and Giemsa solution (Wako).

Western blotting

The adherent hematopoietic cells and OP9 stromal cells were collected, and were then incubated in a new tissue culture dish for 40 min to eliminate adherent OP9 cells. Floating cells were harvested and were subsequently starved in an RPMI1640 medium containing 0.1% FBS and penicillin/streptomycin for 4–6 h. Cells were stimulated with 20 ng/mL TPO for 10 min (for Jak2) or 30 min (for Erk and Akt) before being lyzed in a lysis buffer [20 mM Tris–HCl (pH 8.0), 137 mM NaCl, 1% Triton X-100, 10% glycerol] containing a protease inhibitor cocktail (Sigma) and a phosphatase inhibitor cocktail (Nacalai Tesque). Cell lysates were loaded onto polyacrylamide gels and were transferred to a polyvinylidene fluoride membrane (Millipore). After blocking, the membrane was exposed to mouse anti-phospho-Erk1/2 (Cell Signaling), rabbit anti-Erk1/2 (Sigma), mouse anti-phospho-Akt (Cell Signaling), rabbit anti-total Akt (Cell Signaling), rabbit anti-phospho-Jak2 (Tyr1007/1008; Cell Signaling), or rabbit anti-Jak2 (Cell Signaling), followed by horseradish peroxidase-conjugated secondary antibody. The band was visualized by ECL Plus Western blotting detection reagents (GE Healthcare) or Pierce Western Blotting Substrate Plus (Thermo Scientific), and the signals were read using an LAS-3000 imaging system (Fujifilm).

Reverse transcription–polymerase chain reaction

RT-PCR was carried out as described previously [25]. The sequences of the primers used in this study are listed in Table 1.

Results

Expression of Lnk in mouse ES and iPS cells

We initially investigated Lnk expression in mouse ES cells, iPS cells, ES cell-derived EBs (ES-EBs), and iPS-EBs. As shown in Fig. 1a, Lnk was expressed in undifferentiated ES and iPS cells, and the expression levels of Lnk were significantly increased after EB formation. We further examined whether Lnk was expressed in Flk-1-positive ($^+$) cells, because hematopoietic cells were generated from Flk-1$^+$ cells, a common hemoangiogenic progenitor during ES cell differentiation [29–31]. Quantitative RT-PCR analysis after the purification of Flk-1$^+$ cells from ES-EBs and iPS-EBs revealed that Lnk was highly expressed in Flk-1$^+$ cells (Fig. 1b). These data suggest that Lnk plays some role in the hematopoietic differentiation process in ES and iPS cells.

Enhanced mesodermal differentiation in EB by the inhibition of Lnk

The data described above led to the expectation that hematopoietic cells, including hematopoietic progenitor cells, could be efficiently generated from ES cells and iPS cells by the suppression of Lnk. To inhibit the function of Lnk, we utilized the *DN-Lnk* gene, which was developed by Takizawa et al. [19]. DN-Lnk binds to Lnk, and forms a multimer complex by a homophilic interaction with the N-terminal domain, thereby inhibiting Lnk function [19]. DN-Lnk-expressing ES and iPS cells were generated by introducing a

TABLE 1. LIST OF PRIMERS USED FOR REVERSE TRANSCRIPTION–POLYMERASE CHAIN REACTION

Gene name	*(5′) Sense primers (3′)*	*(5′) Antisense primers (3′)*
Gapdh	ACCACAGTCCATGCCATCAC	TCCACCACCCTGTTGCTGTA
Flk-1	TCTGTGGTTCTGCGTGGAGA	GTATCATTTCCAACCACCC
Lnk	GCCACTTTCTGCAGCTCTTC	GTCCAGGGAGTCAGTGCTTC
Lnk (for real-time)	AGCCACTTTCTGCAGCTCTTC	GTAGAGGTTGTCAGGCATCTCC
DN-Lnk	GGGCTACCAGTGACACCAAT	CACTGTCCACGCTCTGTGAG
Oct-3/4	GTTTGCCAAGCTGCTGAAGC	TCTAGCCCAAGCTGATTGGC
Nanog	ATGGTCTGATTCAGAAGGGC	TTCACCTCCAAATCACTGGC
β-H1	AGTCCCCATGGAGTCAAAGA	CTCAAGGAGACCTTTGCTCA
β-major	CTGACAGATGCTCTCTTGGG	CACAACCCCAGAAACAGACA
Scl/Tal-1	AACAACAACCGGGTGAAGAG	GGGAAAGCACGTCCTGTAGA
Runx1	CTTCCTCTGCTCCGTGCTAC	GACGGCAGAGTAGGGAACTG
Gata1	TTGTGAGGCCAGAGAGTGTG	TTCCTCGTCTGGATTCCATC
Gata2	TAAGCAGAGAAGCAAGGCTCGC	ACAGGCATTGCACAGGTAGTGG
Fli1	CCAACGAACGGAGAGTCATT	ATTCCTTGCCATCCATGTTC
Erg	GGAGCTGTGCAAGATGACAA	GATTAGCAAGGCGGCTACTG
Erg (for real-time)	GGAGTGCAACCCTAGTCAGG	TAGCTGCCGTAGCTCATCC
Sfpi1	CCATAGCGATCACTACTGGGATTT	TGTGAAGTGGTTCTCAGGGAAGT
E47	ATACAGCGAAGGTGCCCACT	CTCAAGGTGCCAACACTGGT

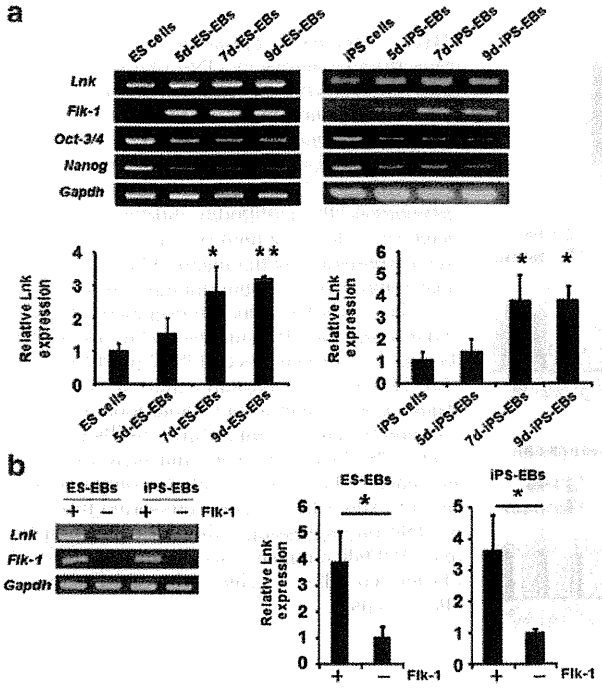

FIG. 1. Lnk is expressed in mouse ES cells, iPS cells, and Flk-1$^+$ hemoangiogenic progenitor cells. **(a)** Total RNA was extracted from undifferentiated ES cells, ES cell-derived EBs cultured for 5, 7, or 9 days (5-day ES-EBs, 7-day ES-EBs, 9-day ES-EBs, respectively), undifferentiated iPS cells, 5-day iPS-EBs, 7-day iPS-EBs, or 9-day iPS-EBs. Then, conventional (*above*) and quantitative (*below*) RT-PCR analysis was carried out. Results shown were the mean of 3 independent experiments with indicated SD. $^*p<0.05$, $^{**}p<0.01$ as compared with undifferentiated ES cells or iPS cells. **(b)** Flk-1$^+$ and Flk-1$^-$ cells were sorted from 7-day ES-EBs or 7-day iPS-EBs using FACSAria. The purity of the Flk-1$^+$ and Flk-1$^-$ cells exceeded 90% and 95%, respectively (data not shown). Total RNA was extracted from both types of cell, and the expression of Lnk was examined by conventional (*left*) and quantitative (*right*) RT-PCR analysis. The data were expressed as mean ± SD ($n=3$); $^*p<0.05$ as compared with Flk-1$^-$ cells. ES, embryonic stem; EBs, embryoid bodies; iPS, induced pluripotent stem; GAPDH, glyceraldehyde-3-phosphate dehydrogenase; RT-PCR, reverse transcription–polymerase chain reaction, SD, standard deviation.

DN-Lnk-expressing plasmid, and *DN-Lnk* mRNA expression was confirmed by RT-PCR (Fig. 2a). In this report, we present data from one DN-Lnk-expressing ES and iPS cell clone, because the same results were obtained from other DN-Lnk-expressing clones. Notably, the expression levels of wild-type Lnk in DN-Lnk-expressing cells were similar to those in *Neo*-expressing cells and their parent cells (Fig. 2a). DN-Lnk-expressing iPS cells maintained the undifferentiated state in culture and possessed pluripotency, as demonstrated by alkaline phosphatase staining, immunostaining, and teratoma formation (Supplementary Fig. S1; Supplementary Data are available online at www.liebertpub.com/scd). Hence, ectopic expression of the *DN-Lnk* gene in ES and iPS cells would not affect their function.

Next, we generated EBs to induce mesodermal cells from DN-Lnk- or *Neo*-expressing ES and iPS cells. EBs were cultured for 7 days, because the proportion of Flk-1$^+$ cells in EBs increased to a peak on day 7, and decreased over the next 2 days in our culture conditions (Supplementary Fig. S2). We found that DN-Lnk-expressing cells on day 7 of the EB culture yielded a modest increase in the number of Flk-1$^+$ hemangiogenic progenitor cells relative to that of *Neo*-expressing cells (Fig. 2b). Interestingly, elevated expression of *Scl/Tal-1*, *Runx1*, and *Gata-1* was observed in DN-Lnk-expressing total EB cells (Fig. 2c). Besides the expression levels of these genes, those of other key transcription factors of blood stem/progenitor cells, including *Gata-2*, *Fli-1*, and *Erg* [32], in DN-Lnk-expressing cells were also upregulated in comparison with those in *Neo*-expressing cells (Fig. 2d). To examine whether increased expression of these transcription factors in DN-Lnk-expressing cells was due to the increased generation of Flk-1$^+$ cells, we performed the gene expression analysis after purification of Flk-1$^+$ cells from DN-Lnk- or *Neo*-expressing total EB cells (Fig. 2e). No difference in the expression of *Runx1*, *Gata-1*, *Gata-2*, *Fli-1*, or *Erg* was observed between DN-Lnk-expressing cells and *Neo*-expressing cells, indicating that elevated expression of these hematopoietic genes in DN-Lnk-expressing EB cells would be largely because of the increased population of Flk-1$^+$ cells. On the other hand, DN-Lnk-expressing Flk-1$^+$ cells showed a 2-fold increase in the expression of *Scl/Tal-1*, an essential transcription factor for the hematopoietic development [33,34], compared with *Neo*-expressing Flk-1$^+$ cells. The increased *Scl/Tal-1* expression thus suggests that an inhibition of Lnk in Flk-1$^+$ cells might contribute to enhance the production of hematopoietic progenitor cells. Taken together, these results raise the possibility that mesodermal cells with a hematopoietic differentiation potential would be efficiently generated in DN-Lnk-expressing cells during EB formation.

Inhibition of Lnk function increases the production of hematopoietic cells

To induce hematopoietic cells, EB-derived cells were cultured on OP9 stromal cells in the presence of hematopoietic cytokines. During culture, cobblestone-forming cells were more frequently observed in DN-Lnk-expressing cells than in *Neo*-expressing cells (Fig. 3a), indicating that DN-Lnk-expressing cells were immature hematopoietic cells with expansion potential. In support of this observation, DN-Lnk-expressing cells showed a significant increase in the number of hematopoietic cells compared to that of *Neo*-expressing cells (Fig. 3b). Importantly, compared to *Neo*-expressing cells, DN-Lnk-expressing cells could more efficiently proliferate on OP9 stromal cells for a period exceeding 14 days (Fig. 3b). Therefore, the proliferation of hematopoietic cells could be augmented by the inhibition of Lnk.

To investigate whether primitive and definitive hematopoiesis could occur in DN-Lnk- or *Neo*-expressing cells, we measured the expression levels of red cell globin by RT-PCR analysis. In both DN-Lnk- and *Neo*-expressing hematopoietic cells, the expression levels of the embryonic globin, *β-H1*, and the adult globin, *β-major*, were decreased and increased, respectively, after culturing on OP9 stromal cells in comparison with those in total EB cells (Fig. 3c). This indicates that DN-Lnk- or *Neo*-expressing cells can show the primitive

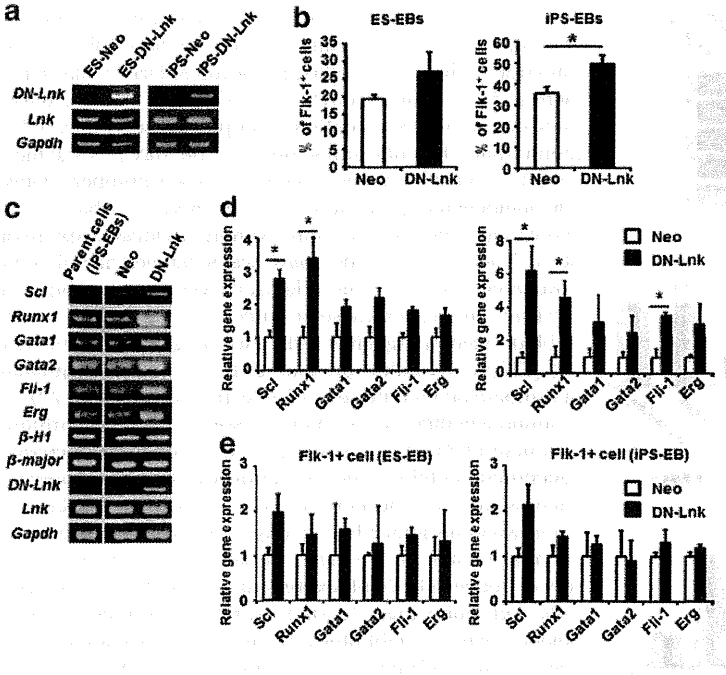

FIG. 2. Increased expression of hematopoietic transcription factors in DN-Lnk-expressing EB cells. **(a)** DN-Lnk-expressing ES cells and iPS cells were generated as described in the Materials and Methods section. DN-Lnk expression was confirmed by RT-PCR. **(b)** EB cells, which were cultured for 7 days, were stained with anti-mouse Flk-1 antibody, and were then subjected to flow cytometric analysis. The data were expressed as the mean ± SD ($n = 3$). **(c)** The expression level of hematopoietic marker genes in 7-day iPS-EBs were investigated by semi-quantitative RT-PCR analysis. The *left panel* indicates the parent iPS cell (38C2)-derived 7-day EBs. **(d)** Gene expression analysis of the key transcription factors of hematopoietic stem/progenitor cells in total 7-day ES-EBs (*left*) and 7-day iPS-EBs (*right*). The data were expressed as mean ± SD ($n = 3$); $^*p < 0.05$ as compared with *Neo*. **(e)** After Flk-1$^+$ cells were sorted from *Neo*- or DN-Lnk-expressing 7-day EB cells, quantitative RT-PCR analysis was performed. *Left*, ES-EB-derived Flk-1$^+$ cells; *right*, iPS-EB-derived Flk-1$^+$ cells.

hematopoiesis followed by definitive hematopoiesis under our culture conditions.

We next examined the colony-forming potential of DN-Lnk-expressing cells. As shown in Fig. 3d, DN-Lnk-expressing cells showed a significant increase in the total colony-forming cell (CFC) number and CFU–granulocyte, macrophage number. Note that the number of CFU-GEMM/CFU-Mix, the most immature multipotent hematopoietic cells, in DN-Lnk-expressing cells was ~5 times as much as that in *Neo*-expressing cells (Fig. 3d). May-Giemsa staining after picking up the colonies revealed that mixed colonies derived from DN-Lnk-expressing cells contained the erythroblasts, granulocytes, macrophages, and megakaryocytes (Fig. 3e), thus confirming the generation of multipotent hematopoietic cells. An elevated CFU-Mix number in DN-Lnk-expressing cells might have been due to the fact that Lnk is highly expressed in immature hematopoietic cells, especially in hematopoietic stem/progenitor cells [13,17]. We also analyzed surface antigen expression in DN-Lnk- or *Neo*-expressing cells by flow cytometry, and found that DN-Lnk-expressing cells showed a higher percentage of CD34$^+$ cells and CD41$^+$ cells (Fig. 3f), suggestive of an increased number of immature hematopoietic cells. In addition, the proportion of CD45$^+$ cells, CD11b$^+$ cells, Gr-1$^+$ cells, or CXCR4$^+$ cells was also increased in DN-Lnk-expressing cells (Fig. 3f). By contrast, a lower percentage of Ter119$^+$ cells were observed in DN-Lnk-expressing cells (Fig. 3f). Consistent with this flow cytometric analysis, we found an increased expression of *Sfpi1* (encoding Pu.1) and *E47*, which are the key factors responsible for hematopoiesis, and a decreased expression of *β-major* globin in DN-Lnk-expressing cells after the cultivation on OP9 stromal cells (Fig. 3c and Supplementary Fig. S3). These results clearly showed that Lnk inhibition promoted the production of hematopoietic cells, including multipotent immature hematopoietic cells and myeloid cells, from mouse ES and iPS cells.

Inhibition of Lnk function in pluripotent stem cell-derived hematopoietic cells augments TPO-mediated signaling

It was previously shown that Lnk negatively regulates various types of hematopoietic cytokine signaling, such as TPO [16]. To investigate whether the increased production of hematopoietic cells from DN-Lnk-expressing cells, described above, is due to the enhanced TPO-mediated signaling, we analyzed protein phosphorylation after TPO stimulation using DN-Lnk-expressing cells. Hematopoietic cells were starved and subsequently stimulated with 20 ng/mL of TPO before the preparation of the cell lysates. The results showed the elevated phosphorylation of Jak2, Erk1/2, and Akt, all of which are downstream of TPO signaling, in DN-Lnk-expressing cells (Fig. 4a). We also found almost no difference in the percentage of Mpl/TPOR-positive cells between DN-Lnk-expressing cells and *Neo*-expressing cells (Fig. 4b), indicating that enhanced TPO signaling in DN-Lnk-expressing cells does not result from the increased percentage of Mpl/TPO-expressing cells. Thus, our data suggest that Lnk inhibition by *DN-Lnk* gene transduction would augment the activation of signaling molecules upon stimulation with cytokines, and thus Lnk inhibition would promote the production of hematopoietic cells in DN-Lnk-expressing cells.

Increased generation of hematopoietic progenitor cells from mouse pluripotent stem cells by transient transduction of a DN-Lnk gene

Our groups have shown that Ad vector-mediated transient, but not constitutive, transduction of differentiation-related genes in pluripotent stem cells could result in the efficient generation of functional cells, such as adipocytes, osteoblasts, hepatocytes, and hematopoietic cells [25,28,35–37]. We expected that the transient inhibition of Lnk in iPS cells could also

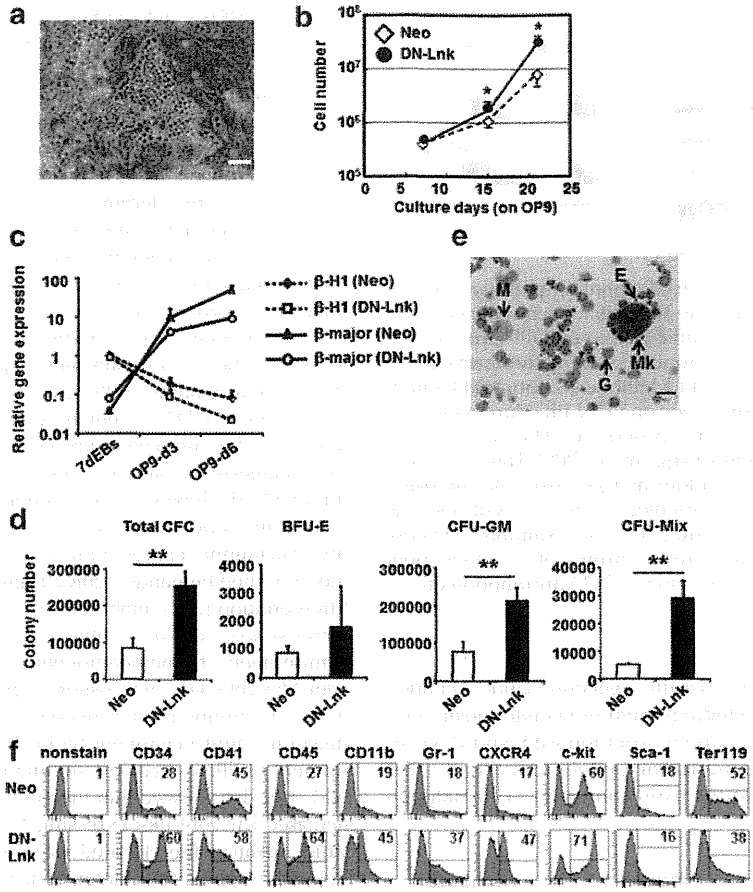

FIG. 3. Efficient generation of hematopoietic cells from iPS cells by overexpression of the *DN-Lnk* gene. EBs derived from *Neo-* or DN-Lnk-expressing iPS cells were cultured for 7 days, and were then plated and cultured on OP9 cells with hematopoietic cytokines to induce and expand the hematopoietic cells. **(a)** Morphology of cobblestone-forming cells derived from DN-Lnk-expressing cells on OP9 stromal cells. Scale bar indicates 100 μm. **(b)** The number of hematopoietic cells was counted on days 7 and 14, after the EB cells were plated on OP9 cells. The data were expressed as mean ± SD ($n = 3$); $^{*}p < 0.05$ as compared with *Neo*. **(c)** Seven-day-cultured EB cells (7-day EBs) were cultured on OP9 cells for 3 or 6 days (OP9-d3 or OP9-d6, respectively). Total RNA was extracted from each cell, and the expression levels of the embryonic *β-H1* globin and the adult *β-major* globin in the cells were measured by real-time PCR. **(d)** After the EB cells had been cultured on OP9 stromal cells for 7 days, the hematopoietic cells were cultured in a methylcellulose-containing medium with hematopoietic cytokines. Ten days later, the number of hematopoietic colonies was then determined using light microscopy. The number of total colonies or subdivided colonies (by morphological subtypes BFU-E, CFU-GM, and CFU-Mix) is shown. The colony number was normalized to the total number of cells. The data were expressed as mean ± SD ($n = 3$); $^{**}p < 0.01$ as compared with *Neo*. **(e)** Cytospin preparation from a DN-Lnk-expressing cell-derived CFU-Mix obtained from the cultures described in **(d)**. E, erythrocyte; G, granulocyte; M, macrophage; Mk, megakaryocyte. Scale bar indicates 30 μm. **(f)** After the EB cells were cocultured with OP9 stromal cells for 14 days, the hematopoietic cells were collected as described in the Materials and Methods section. Hematopoietic cells derived from *Neo-* or DN-Lnk-expressing iPS cells were stained with each antibody, and were then subjected to flow cytometric analysis. The proportion of antigen-positive cells is indicated in the histograms. Representative results from 1 of 3 independent experiments performed are shown. CFC, colony-forming cell; BFU-E, burst-forming unit; CFU-GM, colony-forming unit–granulocyte and monocyte; CFU-Mix/CFU-GEMM, CFU–granulocyte, erythrocyte, monocyte, and megakaryocyte.

accelerate the hematopoietic differentiation. To test this expectation, we generated a DN-Lnk-expressing Ad vector, Ad-DN-Lnk, and examined the effects of transient Lnk inhibition on hematopoietic cell differentiation. The transduction efficiency in EBs, which was transduced with a DsRed-expressing Ad vector, was approximately 40%, as determined by flow cytometry (data not shown). A colony assay after transduction with Ad vectors revealed that the number of total colonies and mixed colonies in the cells transduced with Ad-DN-Lnk was slightly increased in comparison with that in the cells transduced with Ad-LacZ (control vector) (Fig. 5a, c). Moreover, the number of hematopoietic cells increased in Ad-DN-Lnk-transduced cells after 7-day cultivation on OP9 stromal cells (Fig. 5b, d). Thus, our data indicate that the transient inhibition of Lnk also enhances the differentiation and proliferation of hematopoietic cells derived from pluripotent stem cells.

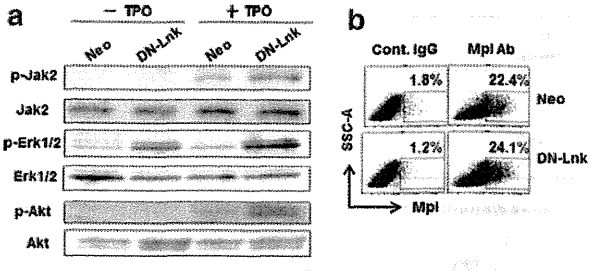

FIG. 4. Enhanced TPO-induced signaling pathway in DN-Lnk-expressing cells. After the EB cells, which were cultured for 7 days, had been plated and cultured on OP9 stromal cells for 14 days, and the hematopoietic cells were harvested as described in the Materials and Methods section. **(a)** Hematopoietic cells derived from *Neo*- or DN-Lnk-expressing cells were starved for 4–6 h in the absence of TPO, and the cells were then stimulated with 20 ng/mL of TPO. Total cell lysates were subjected to western blot analysis using the indicated antibodies. **(b)** After hematopoietic cells were collected, the rate of Mpl/TPOR-expressing cells was examined by flow cytometry. Representative results from 1 of 2 independent experiments performed are shown. TPO, thrombopoietin.

Discussion

In this report, we successfully generated and expanded hematopoietic cells, including immature hematopoietic cells, with colony-forming potential, from mouse ES and iPS cells by the suppression of an adaptor protein Lnk (Fig. 3). We also demonstrated that the expression levels of hematopoietic transcription factors such as *Scl* and *Runx1* in DN-Lnk-expressing total EB cells were significantly increased in comparison with those in *Neo*-expressing total EB cells (Fig. 2c, d), and that cytokine response was augmented in DN-Lnk-expressing cells (Fig. 4). Therefore, the data obtained in this study suggest that Lnk inhibition by enforced expression of a *DN-Lnk* gene in ES and iPS cells would lead both to a promotion of mesodermal differentiation during EB formation and to an increase in the expansion potential of ES and iPS cell-derived hematopoietic cells on an OP9 coculture system, and thus Lnk inhibition could enhance the hematopoietic cell production.

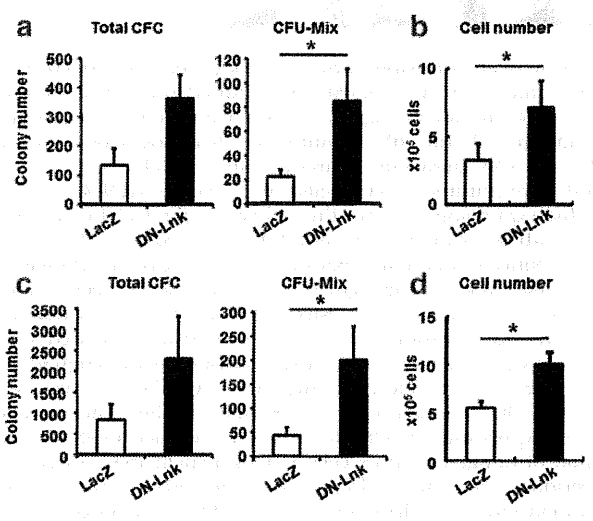

FIG. 5. Expansion of ES cell- and iPS cell-derived hematopoietic cells by the transient expression of DN-Lnk in EB cells. After ES cell- **(a, b)** or iPS cell- **(c, d)** derived EB cells, which were cultured for 7 days, had been transduced with Ad-LacZ or Ad-DN-Lnk at 3,000 VP/cell for 1.5 h, the cells were cultured on OP9 cells with cytokines for 7 days. Hematopoietic cells were collected, and then a colony assay was performed **(a, c)**. The colony number was normalized to the total number of cells. We also counted the number of hematopoietic cells derived from Ad-LacZ- or Ad-DN-Lnk-transduced EB cells **(b, d)**. The data were expressed as mean ± SD ($n = 3$); $^*p < 0.05$ as compared with Ad-LacZ. Ad, adenovirus.

In developing mouse embryos, Lnk is shown to be expressed in the aorta-gonad-mesonephros (AGM) region, the site of hematopoiesis [38]. It has also been reported that the production of $CD45^+$ hematopoietic cells was severely impaired by the enforced expression of Lnk in AGM-derived cells, suggesting that Lnk suppresses hematopoietic commitment [38]. However, the function of Lnk in hematopoiesis is not fully understood. In the current study, we found that Lnk was highly expressed in $Flk\text{-}1^+$ cells (Fig. 1b), which are known to be hemoangiogenic progenitor cells during ES cell differentiation [29]. Furthermore, it was of note that levels of expression of *Scl/Tal-1*, which is essential for hematopoietic commitment of hemoangiogenic progenitor cells derived from ES cells [34], were slightly upregulated in $Flk\text{-}1^+$ cells by the inhibition of Lnk function (Fig. 2e). Thus, it is possible that Lnk might negatively regulate the hematopoietic commitment in $Flk\text{-}1^+$ cells by modulating the expression of *Scl/Tal-1*. We also showed that the percentage of $Flk\text{-}1^+$ cells was increased in DN-Lnk-expressing EB cells (Fig. 2b), and this could result in the elevated expression of other key hematopoietic transcription factors, such as *Runx1* and *Gata-1*, in DN-Lnk-expressing total EB cells compared with that in *Neo*-expressing total EB cells (Fig. 2c, d). This indicates that the functional $Flk\text{-}1^+$ mesodermal cells would be efficiently generated from DN-Lnk-expressing ES and iPS cells. On the other hand, at earlier days of differentiation, the percentage of $CD41^+$ cells, an early hematopoietic progenitor cells generated from pluripotent stem cells [39], in DN-Lnk-expressing EB cells was mostly equal to that in *Neo*-expressing EB cells (Supplementary Fig. S4). Taken together, the findings suggest that Lnk inhibition in ES and iPS cells could be effective for the generation of mesodermal cells with the potential for hematopoietic differentiation, but would not enhance the emergence of hematopoietic progenitor cells at earlier days of EB differentiation.

We examined the cytokine responses of iPS cell-derived hematopoietic cells, and observed the augmented phosphorylation of Erk and Akt in DN-Lnk-expressing cells (Fig. 4). This result is consistent with that of a previous report in which TPO-treated megakaryocytes derived from Lnk-deficient mice enhanced the extent of the activation of Erk and Akt [40]. By contrast, it was reported that Lnk-deficient adult HSCs or bone marrow-derived macrophages showed an enhanced Akt, but not Erk, activation after cytokine stimulation [16,41]. This difference in the activation of downstream molecules is most likely due to differences in cell populations. Because ES cell- and iPS cell-derived hematopoietic cells are heterogeneous, both Akt and Erk phosphorylation levels after cytokine treatment would be augmented in DN-Lnk-expressing cells relative to

Neo-expressing cells. In general, Akt and Erk are known to be involved in cell survival and cell growth [42,43]. Hence, our data indicate that the suppression of Lnk by the ectopic expression of DN-Lnk in ES and iPS cells would lead to an increase in hematopoietic cell production through enhanced cytokine responses.

Recently, Dravid et al. reported the expression of Lnk in human ES cell-derived $CD34^+$ hematopoietic progenitor cells, and they showed that the number of human ES cell-derived $CD34^+$ cells was increased by Lnk knockdown using a lentivirus vector carrying the short-hairpin RNA against Lnk (shLnk) [44]. Their results are mostly consistent with our data, indicating the suppressive function of Lnk in hematopoietic cell generation in both mouse and human pluripotent stem cells. However, the generation of hematopoietic CFCs in shLnk-transduced cells and the molecular mechanisms associated with the generation of $CD34^+$ cells by Lnk knockdown have not been addressed in detail. In this report, we clearly demonstrated that hematopoietic CFCs, including immature multipotent hematopoietic cells, were efficiently generated from mouse ES and iPS cells by Lnk inhibition, and these cells show potential for expansion on OP9 stromal cells (Fig. 3). In addition, we showed that the enhanced generation of hematopoietic cells in DN-Lnk-expressing cells was mediated by the promotion of mesodermal differentiation in EBs and augmented the sensitivity to cytokines in DN-Lnk-expressing cells as described above.

Another important finding of this study was that the transient inhibition of Lnk by Ad vector-mediated transduction of a *DN-Lnk* gene could also be an effective strategy for expanding hematopoietic cells (Fig. 5). Recently, the loss of Lnk and the mutation of Lnk have been reported to be associated with myeloproliferative diseases [45,46], indicating that oncogenesis may result from constitutive Lnk suppression in ES cell- and iPS cell-derived hematopoietic cells via the overexpression of a *DN-Lnk* gene or a lentivirus vector-mediated knockdown system, and such suppression would not be a directly applicable approach for clinical medicine. In this regard, our approaches using Ad vector-mediated transient Lnk inhibition are thought to be quite useful for the safe expansion of the ES cell- and iPS cell-derived hematopoietic cells. However, the number of ES cell- and iPS cell-derived hematopoietic cells in Ad-DN-Lnk-transduced cells was lower than that in the case of stably DN-Lnk-expressing cells (data not shown), possibly due to the low transduction efficiency of Ad vectors in EB cells. Therefore, it will still be necessary to establish methods for transiently inhibiting Lnk functionality using various types of Ad vectors [47] and short interference RNA.

In summary, we successfully developed efficient methods for differentiating mouse ES and iPS cells into hematopoietic cells by the suppression of the adaptor protein Lnk. Lnk functions downstream of multiple hematopoietic cytokine-signaling events, including those involving TPO, SCF, macrophage-colony stimulating factor, and erythropoietin [13,16,40,41,48,49], and Lnk-deficient mice show accumulation of pro-B cells in the bone marrow [48]. Therefore, various types of hematopoietic cells may be efficiently differentiated and expanded from ES and iPS cells by the inhibition of the Lnk function, when an appropriate cytokine is included in the culture; such work is currently ongoing in our laboratory.

Acknowledgments

We thank Misae Nishijima (National Institute of Biomedical Innovation) for her help. We thank Dr. Kazufumi Katayama (Osaka University, Osaka, Japan) for helpful discussion. We also thank Dr. S. Yamanaka and Dr. J. Miyazaki for kindly providing the mouse iPS cell line 38C2 and the CA promoter, respectively. This work was supported by a Grant-in-Aid for Young Scientists (B) (K. Tashiro) of the Ministry of Education, Culture, Sports, Science, and Technology (MEXT) of Japan and the Ministry of Health, Labour, and Welfare of Japan.

Author Disclosure Statement

The authors have no financial conflicts of interest.

References

1. Evans MJ and MH Kaufman. (1981). Establishment in culture of pluripotential cells from mouse embryos. Nature 292:154–156.
2. Thomson JA, J Itskovitz-Eldor, SS Shapiro, MA Waknitz, JJ Swiergiel, VS Marshall and JM Jones. (1998). Embryonic stem cell lines derived from human blastocysts. Science 282:1145–1147.
3. Takahashi K and S Yamanaka. (2006). Induction of pluripotent stem cells from mouse embryonic and adult fibroblast cultures by defined factors. Cell 126:663–676.
4. Takahashi K, K Tanabe, M Ohnuki, M Narita, T Ichisaka, K Tomoda and S Yamanaka. (2007). Induction of pluripotent stem cells from adult human fibroblasts by defined factors. Cell 131:861–872.
5. Nakano T, H Kodama and T Honjo. (1994). Generation of lymphohematopoietic cells from embryonic stem cells in culture. Science 265:1098–1101.
6. Chadwick K, L Wang, L Li, P Menendez, B Murdoch, A Rouleau and M Bhatia. (2003). Cytokines and BMP-4 promote hematopoietic differentiation of human embryonic stem cells. Blood 102:906–915.
7. Schmitt TM, RF de Pooter, MA Gronski, SK Cho, PS Ohashi and JC Zuniga-Pflucker. (2004). Induction of T cell development and establishment of T cell competence from embryonic stem cells differentiated *in vitro*. Nat Immunol 5: 410–417.
8. Hiroyama T, K Miharada, K Sudo, I Danjo, N Aoki and Y Nakamura. (2008). Establishment of mouse embryonic stem cell-derived erythroid progenitor cell lines able to produce functional red blood cells. PLoS One 3:e1544.
9. Choi KD, J Yu, K Smuga-Otto, G Salvagiotto, W Rehrauer, M Vodyanik, J Thomson and I Slukvin. (2009). Hematopoietic and endothelial differentiation of human induced pluripotent stem cells. Stem Cells 27:559–567.
10. Lei F, R Haque, L Weiler, KE Vrana and J Song. (2009). T lineage differentiation from induced pluripotent stem cells. Cell Immunol 260:1–5.
11. Benezra R, RL Davis, D Lockshon, DL Turner and H Weintraub. (1990). The protein Id: a negative regulator of helix-loop-helix DNA binding proteins. Cell 61:49–59.
12. Hong SH, JH Lee, JB Lee, J Ji and M Bhatia. (2011). ID1 and ID3 represent conserved negative regulators of human embryonic and induced pluripotent stem cell hematopoiesis. J Cell Sci 124:1445–1452.
13. Takaki S, H Morita, Y Tezuka and K Takatsu. (2002). Enhanced hematopoiesis by hematopoietic progenitor cells

lacking intracellular adaptor protein, Lnk. J Exp Med 195: 151–160.
14. Velazquez L, AM Cheng, HE Fleming, C Furlonger, S Vesely, A Bernstein, CJ Paige and T Pawson. (2002). Cytokine signaling and hematopoietic homeostasis are disrupted in Lnk-deficient mice. J Exp Med 195:1599–1611.
15. Ema H, K Sudo, J Seita, A Matsubara, Y Morita, M Osawa, K Takatsu, S Takaki and H Nakauchi. (2005). Quantification of self-renewal capacity in single hematopoietic stem cells from normal and Lnk-deficient mice. Dev Cell 8:907–914.
16. Seita J, H Ema, J Ooehara, S Yamazaki, Y Tadokoro, A Yamasaki, K Eto, S Takaki, K Takatsu and H Nakauchi. (2007). Lnk negatively regulates self-renewal of hematopoietic stem cells by modifying thrombopoietin-mediated signal transduction. Proc Natl Acad Sci U S A 104:2349–2354.
17. Kwon SM, T Suzuki, A Kawamoto, M Ii, M Eguchi, H Akimaru, M Wada, T Matsumoto, H Masuda, et al. (2009). Pivotal role of lnk adaptor protein in endothelial progenitor cell biology for vascular regeneration. Circ Res 104:969–977.
18. Yokota Y. (2001). Id and development. Oncogene 20:8290–8298.
19. Takizawa H, C Kubo-Akashi, I Nobuhisa, SM Kwon, M Iseki, T Taga, K Takatsu and S Takaki. (2006). Enhanced engraftment of hematopoietic stem/progenitor cells by the transient inhibition of an adaptor protein, Lnk. Blood 107: 2968–2975.
20. Mizuguchi H and MA Kay. (1998). Efficient construction of a recombinant adenovirus vector by an improved *in vitro* ligation method. Hum Gene Ther 9:2577–2583.
21. Mizuguchi H and MA Kay. (1999). A simple method for constructing E1- and E1/E4-deleted recombinant adenoviral vectors. Hum Gene Ther 10:2013–2017.
22. Kawabata K, F Sakurai, T Yamaguchi, T Hayakawa and H Mizuguchi. (2005). Efficient gene transfer into mouse embryonic stem cells with adenovirus vectors. Mol Ther 12: 547–554.
23. Niwa H, K Yamamura and J Miyazaki. (1991). Efficient selection for high-expression transfectants with a novel eukaryotic vector. Gene 108:193–199.
24. Tashiro K, K Kawabata, H Sakurai, S Kurachi, F Sakurai, K Yamanishi and H Mizuguchi. (2008). Efficient adenovirus vector-mediated PPAR gamma gene transfer into mouse embryoid bodies promotes adipocyte differentiation. J Gene Med 10:498–507.
25. Tashiro K, K Kawabata, M Omori, T Yamaguchi, F Sakurai, K Katayama, T Hayakawa and H Mizuguchi. (2012). Promotion of hematopoietic differentiation from mouse induced pluripotent stem cells by transient HoxB4 transduction. Stem Cell Res 8:300–311.
26. Maizel JV, Jr., DO White and MD Scharff. (1968). The polypeptides of adenovirus. I. Evidence for multiple protein components in the virion and a comparison of types 2, 7A, and 12. Virology 36:115–125.
27. Okita K, T Ichisaka and S Yamanaka. (2007). Generation of germline-competent induced pluripotent stem cells. Nature 448:313–317.
28. Tashiro K, M Inamura, K Kawabata, F Sakurai, K Yamanishi, T Hayakawa and H Mizuguchi. (2009). Efficient adipocyte and osteoblast differentiation from mouse induced pluripotent stem cells by adenoviral transduction. Stem Cells 27:1802–1811.
29. Nishikawa SI, S Nishikawa, M Hirashima, N Matsuyoshi and H Kodama. (1998). Progressive lineage analysis by cell sorting and culture identifies FLK1+VE-cadherin+ cells at a diverging point of endothelial and hemopoietic lineages. Development 125:1747–1757.
30. Yamashita J, H Itoh, M Hirashima, M Ogawa, S Nishikawa, T Yurugi, M Naito and K Nakao. (2000). Flk1-positive cells derived from embryonic stem cells serve as vascular progenitors. Nature 408:92–96.
31. Huber TL, V Kouskoff, HJ Fehling, J Palis and G Keller. (2004). Haemangioblast commitment is initiated in the primitive streak of the mouse embryo. Nature 432:625–630.
32. Wilson NK, SD Foster, X Wang, K Knezevic, J Schutte, P Kaimakis, PM Chilarska, S Kinston, WH Ouwehand et al. (2010). Combinatorial transcriptional control in blood stem/progenitor cells: genome-wide analysis of ten major transcriptional regulators. Cell Stem Cell 7:532–544.
33. Robb L, NJ Elwood, AG Elefanty, F Kontgen, R Li, LD Barnett and CG Begley. (1996). The scl gene product is required for the generation of all hematopoietic lineages in the adult mouse. EMBO J 15:4123–4129.
34. D'Souza SL, AG Elefanty and G Keller. (2005). SCL/Tal-1 is essential for hematopoietic commitment of the hemangioblast but not for its development. Blood 105:3862–3870.
35. Inamura M, K Kawabata, K Takayama, K Tashiro, F Sakurai, K Katayama, M Toyoda, H Akutsu, Y Miyagawa, et al. (2011). Efficient generation of hepatoblasts from human ES cells and iPS cells by transient overexpression of homeobox gene HEX. Mol Ther 19:400–407.
36. Takayama K, M Inamura, K Kawabata, K Tashiro, K Katayama, F Sakurai, T Hayakawa, Furue MK, H Mizuguchi. (2011). Efficient and directive generation of two distinct endoderm lineages from human ESCs and iPSCs by differentiation stage-specific SOX17 transduction. PLoS One 6: e21780.
37. Takayama K, M Inamura, K Kawabata, K Katayama, M Higuchi, K Tashiro, A Nonaka, F Sakurai, T Hayakawa, F Kusudaurue M and H Mizuguchi. (2012). Efficient generation of functional hepatocytes from human embryonic stem cells and induced pluripotent stem cells by HNF4alpha transduction. Mol Ther 20:127–137.
38. Nobuhisa I, M Takizawa, S Takaki, H Inoue, K Okita, M Ueno, K Takatsu and T Taga. (2003). Regulation of hematopoietic development in the aorta-gonad-mesonephros region mediated by Lnk adaptor protein. Mol Cell Biol 23: 8486–8494.
39. Matsumoto K, T Isagawa, T Nishimura, T Ogaeri, K Eto, S Miyazaki, J Miyazaki, H Aburatani, H Nakauchi and H Ema. (2009). Stepwise development of hematopoietic stem cells from embryonic stem cells. PLoS One 4:e4820.
40. Tong W and HF Lodish. (2004). Lnk inhibits Tpo-mpl signaling and Tpo-mediated megakaryocytopoiesis. J Exp Med 200:569–580.
41. Gueller S, HS Goodridge, B Niebuhr, H Xing, M Koren Michowitz, H Serve, DM Underhill, CH Brandts and HP Koeffler. (2010). Adaptor protein Lnk inhibits c-Fms-mediated macrophage function. J Leukoc Biol 88:699–706.
42. Geest CR and PJ Coffer. (2009). MAPK signaling pathways in the regulation of hematopoiesis. J Leukoc Biol 86:237–250.
43. Martelli AM, C Evangelisti, F Chiarini, C Grimaldi, A Cappellini, A Ognibene and JA McCubrey. (2010). The emerging role of the phosphatidylinositol 3-kinase/Akt/mammalian target of rapamycin signaling network in normal myelopoiesis and leukemogenesis. Biochim Biophys Acta 1803: 991–1002.
44. Dravid G, Y Zhu, J Scholes, D Evseenko and GM Crooks. (2011). Dysregulated gene expression during hematopoietic

differentiation from human embryonic stem cells. Mol Ther 19:768–781.
45. Bersenev A, C Wu, J Balcerek, J Jing, M Kundu, GA Blobel, KR Chikwava and W Tong. (2010). Lnk constrains myeloproliferative diseases in mice. J Clin Invest 120:2058–2069.
46. Oh ST, EF Simonds, C Jones, MB Hale, Y Goltsev, KD Gibbs, Jr., JD Merker, JL Zehnder, GP Nolan and J Gotlib. (2010). Novel mutations in the inhibitory adaptor protein LNK drive JAK-STAT signaling in patients with myeloproliferative neoplasms. Blood 116:988–992.
47. Kawabata K, F Sakurai, N Koizumi, T Hayakawa and H Mizuguchi. (2006). Adenovirus vector-mediated gene transfer into stem cells. Mol Pharm 3:95–103.
48. Takaki S, K Sauer, BM Iritani, S Chien, Y Ebihara, K Tsuji, K Takatsu and RM Perlmutter. (2000). Control of B cell production by the adaptor protein lnk. Definition Of a conserved family of signal-modulating proteins. Immunity 13:599–609.
49. Tong W, J Zhang and HF Lodish. (2005). Lnk inhibits erythropoiesis and Epo-dependent JAK2 activation and downstream signaling pathways. Blood 105:4604–4612.

Address correspondence to:
Dr. Hiroyuki Mizuguchi
Laboratory of Biochemistry and Molecular Biology
Graduate School of Pharmaceutical Sciences
Osaka University
1-6 Yamadaoka, Suita
Osaka 565-0871
Japan

E-mail: mizuguch@phs.osaka-u.ac.jp

Received for publication February 27, 2012
Accepted after revision June 27, 2012
Prepublished on Leibert Instant Online June 28, 2012

Research Article

EASL EUROPEAN ASSOCIATION FOR THE STUDY OF THE LIVER | JOURNAL OF HEPATOLOGY

Generation of metabolically functioning hepatocytes from human pluripotent stem cells by FOXA2 and HNF1α transduction

Kazuo Takayama[1,2], Mitsuru Inamura[1,2], Kenji Kawabata[2,3], Michiko Sugawara[4], Kiyomi Kikuchi[4], Maiko Higuchi[2], Yasuhito Nagamoto[1,2], Hitoshi Watanabe[1,2], Katsuhisa Tashiro[2], Fuminori Sakurai[1], Takao Hayakawa[5,6], Miho Kusuda Furue[7,8], Hiroyuki Mizuguchi[1,2,9,*]

[1]*Laboratory of Biochemistry and Molecular Biology, Graduate School of Pharmaceutical Sciences, Osaka University, Osaka 565-0871, Japan;* [2]*Laboratory of Stem Cell Regulation, National Institute of Biomedical Innovation, Osaka 567-0085, Japan;* [3]*Laboratory of Biomedical Innovation, Graduate School of Pharmaceutical Sciences, Osaka University, Osaka 565-0871, Japan;* [4]*Tsukuba Laboratories, Eisai Co., Ltd., Ibaraki 300-2635, Japan;* [5]*Pharmaceutics and Medical Devices Agency, Tokyo 100-0013, Japan;* [6]*Pharmaceutical Research and Technology Institute, Kinki University, Osaka 577-8502, Japan;* [7]*Laboratory of Cell Cultures, Department of Disease Bioresources Research, National Institute of Biomedical Innovation, Osaka 567-0085, Japan;* [8]*Laboratory of Cell Processing, Institute for Frontier Medical Sciences, Kyoto University, Kyoto 606-8507, Japan;* [9]*The Center for Advanced Medical Engineering and Informatics, Osaka University, Osaka 565-0871, Japan*

Background & Aims: Hepatocyte-like cells differentiated from human embryonic stem cells (hESCs) and induced pluripotent stem cells (hiPSCs) can be utilized as a tool for screening for hepatotoxicity in the early phase of pharmaceutical development. We have recently reported that hepatic differentiation is promoted by sequential transduction of SOX17, HEX, and HNF4α into hESC- or hiPSC-derived cells, but further maturation of hepatocyte-like cells is required for widespread use of drug screening.
Methods: To screen for hepatic differentiation-promoting factors, we tested the seven candidate genes related to liver development.
Results: The combination of two transcription factors, FOXA2 and HNF1α, promoted efficient hepatic differentiation from hESCs and hiPSCs. The expression profile of hepatocyte-related genes (such as genes encoding cytochrome P450 enzymes, conjugating enzymes, hepatic transporters, and hepatic nuclear receptors) achieved with FOXA2 and HNF1α transduction was comparable to that obtained in primary human hepatocytes. The hepatocyte-like cells generated by FOXA2 and HNF1α transduction exerted various hepatocyte functions including albumin and urea secretion, and the uptake of indocyanine green and low density lipoprotein. Moreover, these cells had the capacity to metabolize all nine tested drugs and were successfully employed to evaluate drug-induced cytotoxicity.
Conclusions: Our method employing the transduction of FOXA2 and HNF1α represents a useful tool for the efficient generation of metabolically functional hepatocytes from hESCs and hiPSCs, and the screening of drug-induced cytotoxicity.

Keywords: FOXA2; HNF1α; Hepatocytes; Adenovirus; Drug screening; Drug metabolism; hESCs; hiPSCs.
Received 14 November 2011; received in revised form 31 March 2012; accepted 4 April 2012; available online 29 May 2012
* Corresponding author. Address: Laboratory of Biochemistry and Molecular Biology, Graduate School of Pharmaceutical Sciences, Osaka University, 1-6 Yamadaoka, Suita, Osaka 565-0871, Japan. Tel.: +81 6 6879 8185; fax: +81 6 6879 8186.
E-mail address: mizuguch@phs.osaka-u.ac.jp (H. Mizuguchi).

Introduction

Hepatocyte-like cells differentiated from human embryonic stem cells (hESCs) [1] or human induced pluripotent stem cells (hiPSCs) [2] have more advantages than primary human hepatocytes (PHs) for drug screening. While application of PHs in drug screening has been hindered by lack of cellular growth, loss of function, and de-differentiation *in vitro* [3], hESC- or hiPSC-derived hepatocyte-like cells (hESC-hepa or hiPSC-hepa, respectively) have potential to solve these problems.

Hepatic differentiation from hESCs and hiPSCs can be divided into four stages: definitive endoderm (DE) differentiation, hepatic commitment, hepatic expansion, and hepatic maturation. Various growth factors are required to mimic liver development [4] and to promote hepatic differentiation. Previously, we showed that transduction of transcription factors in addition to treatment with optimal growth factors was effective to enhance hepatic differentiation [5–7]. An almost homogeneous hepatocyte population was obtained by sequential transduction of SOX17, HEX, and HNF4α into hESC- or hiPSCs-derived cells [7]. However, further maturation of the hESC-hepa and hiPSC-hepa is required for widespread use of drug screening because the drug metabolism capacity of these cells was not sufficient.

In some previous reports, hESC-hepa and hiPSC-hepa have been characterized for their hepatocyte functions in numerous ways, including functional assessment such as glycogen storage and low density lipoprotein (LDL) uptake [7]. To make a more precise judgment as to whether hESC-hepa and hiPSC-hepa can be applied to drug screening, it is more important to assess cytochrome P450 (CYP) induction potency and drug metabolism capacity rather than general hepatocyte function. Although Duan *et al.* have examined the drug metabolism capacity of hESC-hepa, drug metabolites were measured at 24 or 48 h [8]. To precisely

estimate the drug metabolism capacity, the amount of metabolites must be measured during the time when production of metabolites is linearly detected (generally before 24 h). To the best of our knowledge, there have been few reports that have examined various drugs metabolism capacity of hESC-hepa and hiPSC-hepa in detail.

In the present study, seven candidate genes (*FOXA2*, *HEX*, *HNF1α*, *HNF1β*, *HNF4α*, *HNF6*, and *SOX17*) were transduced into each stage of hepatic differentiation from hESCs by using an adenovirus (Ad) vector to screen for hepatic differentiation-promoting factors. Then, hepatocyte-related gene expression profiles and hepatocyte functions in hESC-hepa and hiPSC-hepa generated by the optimized protocol, were examined to investigate whether these cells have PHs characteristics. We used nine drugs, which are metabolized by various CYP enzymes and UDP-glucuronosyltransferases (UGTs), to determine whether the hESC-hepa and hiPSC-hepa have drug metabolism capacity. Furthermore, hESC-hepa and hiPSC-hepa were examined to determine whether these cells may be applied to evaluate drug-induced cytotoxicity.

Materials and methods

In vitro differentiation

Before the initiation of cellular differentiation, the medium of hESCs and hiPSCs was exchanged for a defined serum-free medium, hESF9, and cultured as previously reported [9]. The differentiation protocol for the induction of DE cells, hepatoblasts, and hepatocytes was based on our previous report with some modifications [5,6]. Briefly, in mesendoderm differentiation, hESCs and hiPSCs were dissociated into single cells by using Accutase (Millipore) and cultured for 2 days on Matrigel (BD biosciences) in differentiation hESF-DIF medium which contains 100 ng/ml Activin A (R&D Systems) and 10 ng/ml bFGF (hESF-DIF medium, Cell Science & Technology Institute; differentiation hESF-DIF medium was supplemented with 10 μg/ml human recombinant insulin, 5 μg/ml human apotransferrin, 10 μM 2-mercaptoethanol, 10 μM ethanolamine, 10 μM sodium selenite, and 0.5 mg/ml bovine serum albumin, all from Sigma). To generate DE cells, mesendoderm cells were transduced with 3000 VP/cell of Ad-FOXA2 for 1.5 h on day 2 and cultured until day 6 on Matrigel in differentiation hESF-DIF medium supplemented with 100 ng/ml Activin A and 10 ng/ml bFGF. For induction of hepatoblasts, the DE cells were transduced with each 1500 VP/cell of Ad-FOXA2 and Ad-HNF1α for 1.5 h on day 6 and cultured for 3 days on Matrigel in hepatocyte culture medium (HCM, Lonza) supplemented with 30 ng/ml bone morphogenetic protein 4 (BMP4, R&D Systems) and 20 ng/ml FGF4 (R&D Systems). In hepatic expansion, the hepatoblasts were transduced with each 1500 VP/cell of Ad-FOXA2 and Ad-HNF1α for 1.5 h on day 9 and cultured for 3 days on Matrigel in HCM supplemented with 10 ng/ml hepatocyte growth factor (HGF), 10 ng/ml FGF1, 10 ng/ml FGF4, and 10 ng/ml FGF10 (all from R&D Systems). In hepatic maturation, cells were cultured for 8 days on Matrigel in L15 medium (Invitrogen) supplemented with 8.3% tryptose phosphate broth (BD biosciences), 10% FBS (Vita), 10 μM hydrocortisone 21-hemisuccinate (Sigma), 1 μM insulin, 25 mM $NaHCO_3$ (Wako), 20 ng/ml HGF, 20 ng/ml Oncostatin M (OsM, R&D systems), and 10^{-6} M Dexamethasone (DEX, Sigma).

Results

Recently, we showed that the sequential transduction of SOX17, HEX, and HNF4α into hESC-derived mesendoderm, DE, and hepatoblasts, respectively, leads to efficient generation of the hESC-hepa [5–7]. In the present study, to further improve the differentiation efficiency towards hepatocytes, we screened for hepatic differentiation-promoting transcription factors. Seven candidate genes involved in liver development were selected. We then examined the function of the hESC-hepa and hiPSC-hepa generated by the optimized protocol for pharmaceutical use in detail.

Efficient hepatic differentiation by Ad-FOXA2 and Ad-HNF1α transduction

To perform efficient DE differentiation, T-positive hESC-derived mesendoderm cells (day 2) (Supplementary Fig. 1) were transduced with Ad vector expressing various transcription factors (Ad-FOXA2, Ad-HEX, Ad-HNF1α, Ad-HNF1β, Ad-HNF4α, Ad-HNF6, and Ad-SOX17 were used in this study). We ascertained the expression of *FOXA2*, *HEX*, *HNF1α*, *HNF1β*, *HNF4α*, *HNF6*, or *SOX17* in Ad-FOXA2-, Ad-HEX-, Ad-HNF1α-, Ad-HNF1β-, Ad-HNF4α-, Ad-HNF6-, or Ad-SOX17-transduced cells, respectively (Supplementary Fig. 2). We also verified that there was no cytotoxicity of the cells transduced with Ad vector until the total amount of Ad vector reached 12,000 VP/cell (Supplementary Fig. 3). Each transcription factor was expressed in hESC-derived mesendoderm cells on day 2 by using Ad vector, and the efficiency of DE differentiation was examined (Fig. 1A). The DE differentiation efficiency based on CXCR4-positive cells was the highest when Ad-SOX17 or Ad-FOXA2 were transduced (Fig. 1B). To investigate the difference between Ad-FOXA2-transduced cells and Ad-SOX17-transduced cells, gene expression levels of markers of undifferentiated cells, mesendoderm cells, DE cells, and extraembryonic endoderm cells were examined (Fig. 1C). The expression levels of extraembryonic endoderm markers of Ad-SOX17-transduced cells were higher than those of Ad-FOXA2-transduced cells. Therefore, we concluded that FOXA2 transduction is suitable for use in selective DE differentiation.

To promote hepatic commitment, various transcription factors were transduced into DE cells and the resulting phenotypes were examined on day 9 (Fig. 1D). Nearly 100% of the population of Ad-FOXA2-transduced cells and Ad-HNF1α-transduced cells was α-fetoprotein (AFP)-positive (Fig. 1E). We expected that hepatic commitment would be further accelerated by combining FOXA2 and HNF1α transduction. The DE cells were transduced with both Ad-FOXA2 and Ad-HNF1α, and then the gene expression levels of *CYP3A7* [10], which is a marker of fetal hepatocytes, were evaluated (Fig. 1F). When both Ad-FOXA2 and Ad-HNF1α were transduced into DE cells, the promotion of hepatic commitment was greater than in Ad-FOXA2-transduced cells or Ad-HNF1α-transduced cells.

To promote hepatic expansion and maturation, we transduced various transcription factors into hepatoblasts on day 9 and 12 and the resulting phenotypes were examined on day 20 (Fig. 1G). We ascertained that the hepatoblast population was efficiently expanded by addition of HGF, FGF1, FGF4, and FGF10 (Supplementary Fig. 4). The hepatic differentiation efficiency based on asialoglycoprotein receptor 1 (ASGR1)-positive cells was measured on day 20, demonstrating that FOXA2, HNF1α, and HNF4α transduction could promote efficient hepatic maturation (Fig. 1H). To investigate the phenotypic difference between Ad-FOXA2-, Ad-HNF1α-, and Ad-HNF4α-transduced cells, gene expression levels of early hepatic markers, mature hepatic markers, and biliary markers were examined (Fig. 1I). Gene expression levels of mature hepatic markers were up-regulated by FOXA2, HNF1α, or HNF4α transduction. FOXA2 transduction strongly upregulated gene expression levels of both early hepatic markers and mature hepatic markers, while HNF1α or HNF4α transduc-

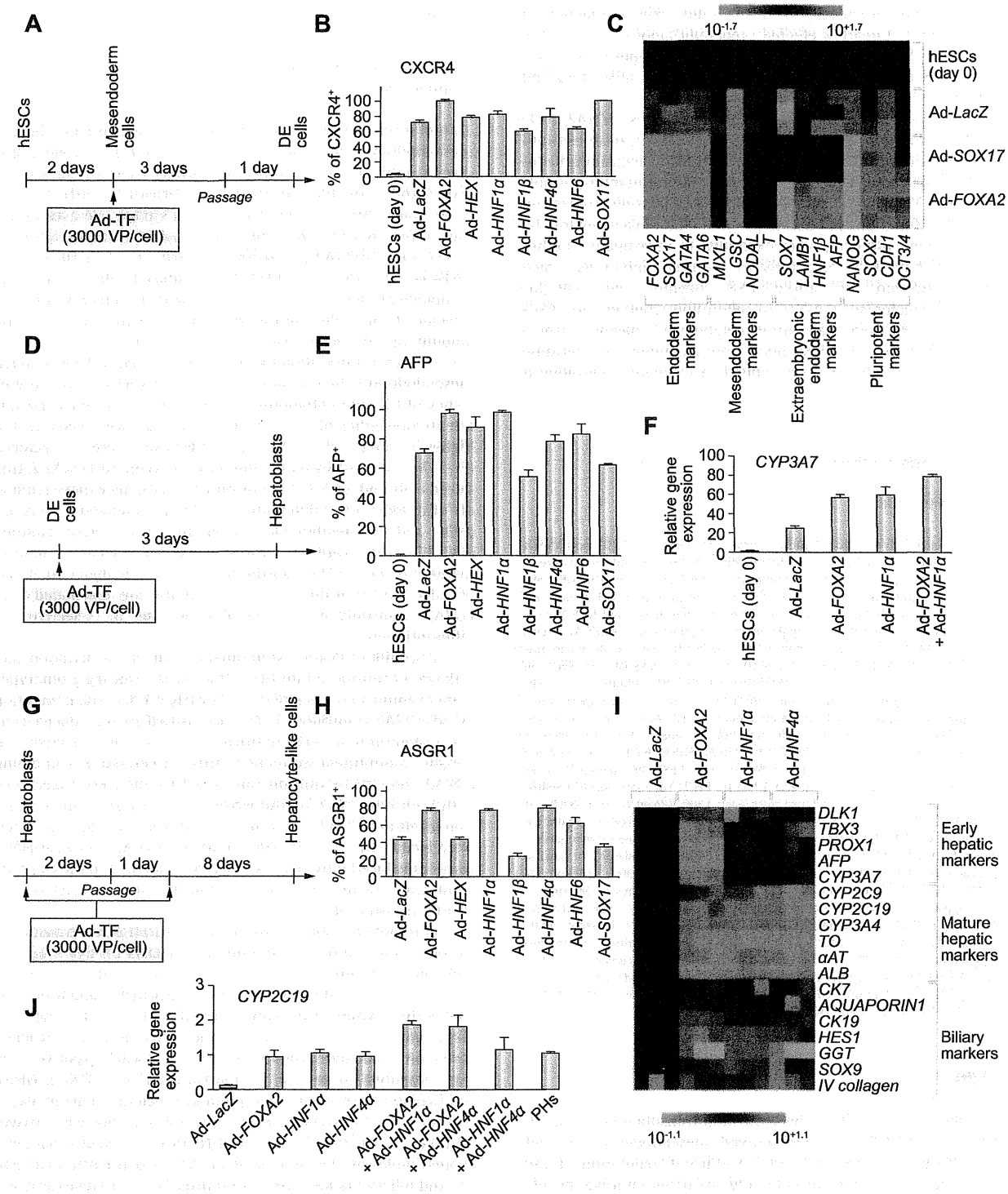

Fig. 1. Efficient hepatic differentiation from hESCs by FOXA2 and HNF1α transduction. (A) The schematic protocol describes the strategy for DE differentiation from hESCs (H9). Mesendoderm cells (day 2) were transduced with 3000 VP/cell of transcription factor (TF)-expressing Ad vector (Ad-TF) for 1.5 h and cultured as described in Fig. 2A. (B) On day 5, the efficiency of DE differentiation was measured by estimating the percentage of CXCR4-positive cells using FACS analysis. (C) The gene expression profiles were examined on day 5. (D) Schematic protocol describing the strategy for hepatoblast differentiation from DE. DE cells (day 6) were transduced with 3000 VP/cell of Ad-TF for 1.5 h and cultured as described in Fig. 2A. (E) On day 9, the efficiency of hepatoblast differentiation was measured by estimating the percentage of AFP-positive

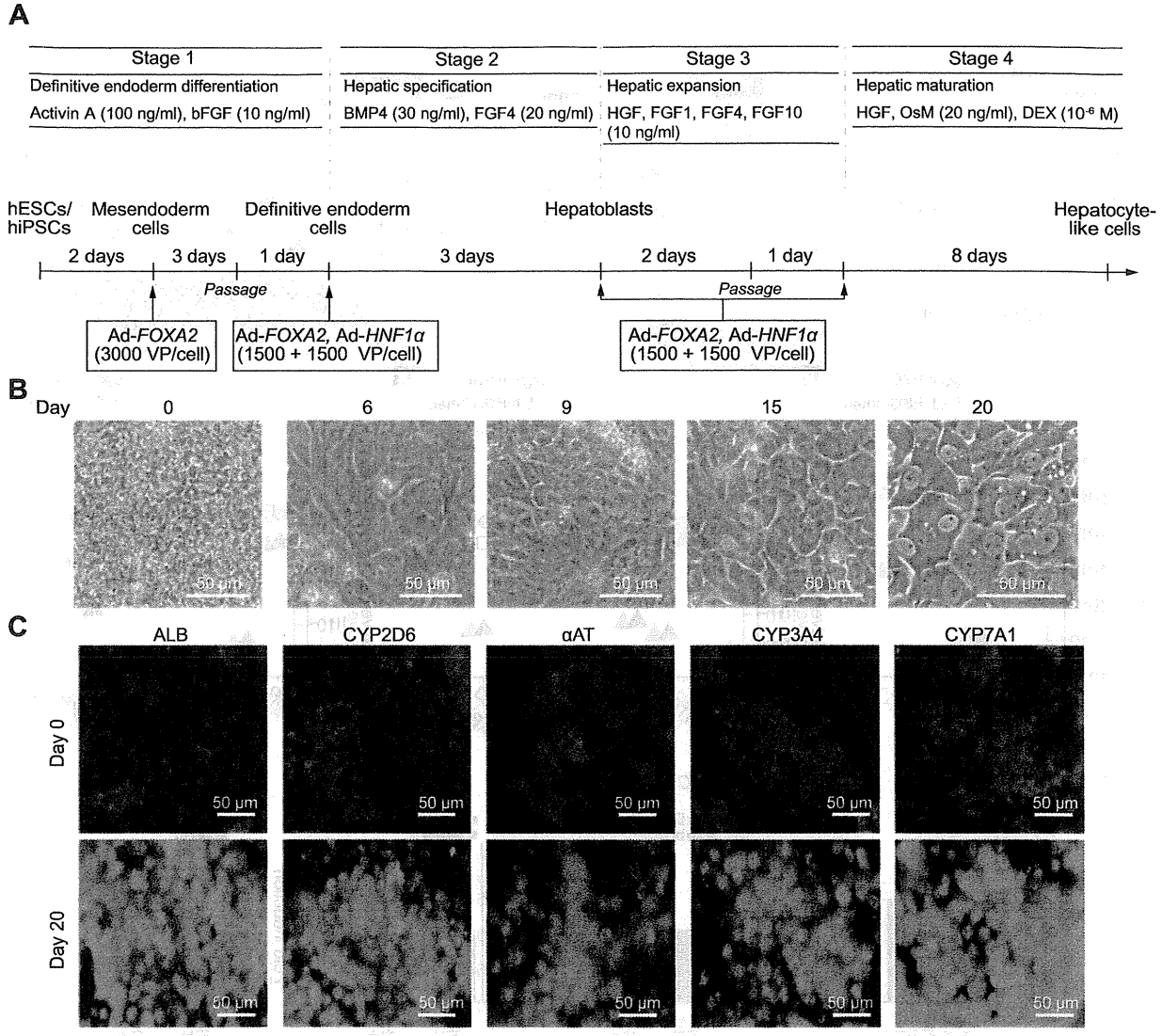

Fig. 2. Hepatic differentiation of hESCs and hiPSCs by FOXA2 and HNF1α transduction. (A) The differentiation procedure of hESCs and hiPSCs into hepatocytes via DE cells and hepatoblasts is schematically shown. Details of the hepatic differentiation procedure are described in Materials and methods. (B) Sequential morphological changes (day 0–20) of hESCs (H9) differentiated into hepatocytes are shown. (C) The expression of the hepatocyte markers (ALB, CYP2D6, αAT, CYP3A4, and CYP7A1, all green) was examined by immunohistochemistry on day 0 and 20. Nuclei were counterstained with DAPI (blue).

tion did not up-regulate the gene expression levels of early hepatic markers. Next, multiple transduction of transcription factors was performed to promote further hepatic maturation. The combination of Ad-FOXA2 and Ad-HNF1α transduction and the combination of Ad-FOXA2 and Ad-HNF4α transduction result in the most efficient hepatic maturation, judged from the gene expression levels of *CYP2C19* (Fig. 1J). This may happen because the mixture of immature hepatocytes and mature hepatocytes coor-

cells using FACS analysis. (F) The gene expression level of *CYP3A7* was measured by real-time RT-PCR on day 9. On the *y* axis, the gene expression level of *CYP3A7* in hESCs (day 0) was taken as 1.0. (G) The schematic protocol describes the strategy for hepatic differentiation from hepatoblasts. Hepatoblasts (day 9) were transduced with 3000 VP/cell of Ad-TF for 1.5 h and cultured as described in Fig. 2A. (H) On day 20, the efficiency of hepatic differentiation was measured by estimating the percentage of ASGR1-positive cells using FACS analysis. The detail results of FACS analysis are shown in Supplementary Table 1. (I) Gene expression profiles were examined on day 20. (J) Hepatoblasts (day 9) were transduced with 3000 VP/cell of Ad-TFs (in the case of combination transduction of two types of Ad vector, 1500 VP/cell of each Ad-TF was transduced) for 1.5 h and cultured. Gene expression levels of *CYP2C19* were measured by real-time RT-PCR on day 20. On the *y* axis, the gene expression level of *CYP2C19* in PHs, which were cultured for 48 h after the cells were plated, was taken as 1.0. All data are represented as mean ± SD (n = 3).

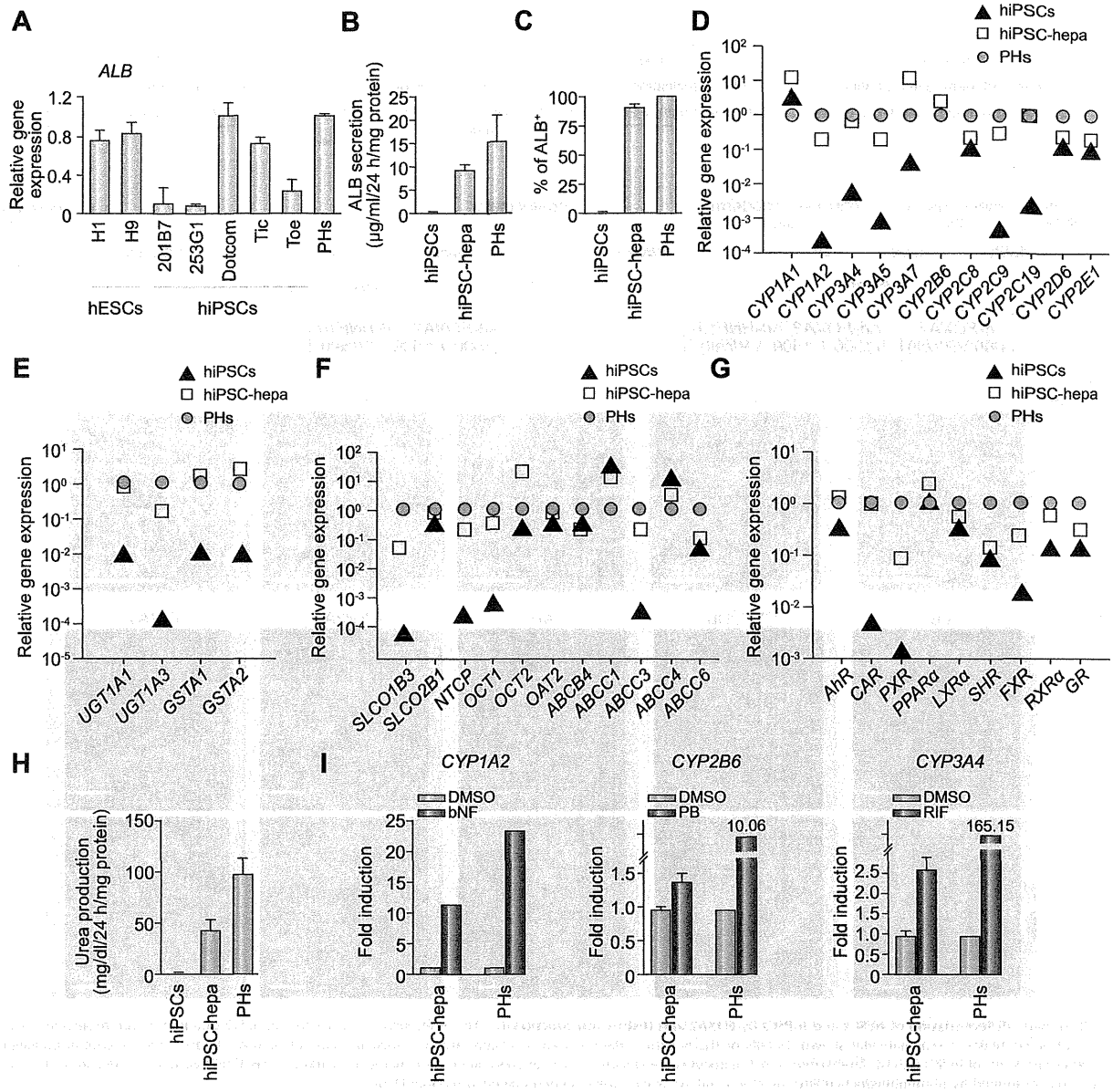

Fig. 3. The hepatic characterization of hiPSC-hepa. hESCs (H1 and H9) and hiPSCs (201B7, 253G1, Dotcom, Tic, and Toe) were differentiated into hepatocyte-like cells as described in Fig. 2A. (A) On day 20, the gene expression level of *ALB* was examined by real-time RT-PCR. On the *y* axis, the gene expression level of *ALB* in PHs, which were cultured for 48 h after cells were plated, was taken as 1.0. (B–I) hiPSCs (Dotcom) were differentiated into hepatocyte-like cells as described in Fig. 2A. (B) The amount of ALB secretion was examined by ELISA in hiPSCs, hiPSC-hepa, and PHs. (C) hiPSCs, hiPSC-hepa, and PHs were subjected to immunostaining with anti-ALB antibodies, and then the percentage of ALB-positive cells was examined by flow cytometry. (D–G) The gene expression levels of CYP enzymes (D), conjugating enzymes (E), hepatic transporters (F), and hepatic nuclear receptors (G) were examined by real-time RT-PCR in hiPSCs, hiPSC-hepa, and PHs. On the *y* axis, the expression level of PHs is indicated. (H) The amount of urea secretion was examined in hiPSCs, hiPSC-hepa, and PHs. (I) Induction of *CYP1A2*, *2B6*, or *3A4* by DMSO or inducer (bNF, PB, or RIF) of hiPSC-hepa and PHs, cultured for 48 h after the cells were plated, was examined. On the y axis, the gene expression levels of *CYP1A2*, *2B6*, or *3A4* in DMSO-treated cells, which were cultured for 48 h, were taken as 1.0. All data are represented as mean ± SD (n = 3).

dinately works to induce hepatocyte functions. Taken together, efficient hepatic differentiation could be promoted by using the combination of FOXA2 and HNF1α transduction at the optimal stage of differentiation (Fig. 2A). At the stage of hepatic expansion and maturation, Ad-HNF4α can be substituted for Ad-HNF1α (Fig. 1J). Interestingly, cell growth was delayed by FOXA2 and HNF4α transduction (Supplementary Fig. 5). This delay in cell proliferation might be due to promoted maturation by FOXA2 and HNF1α transduction. As the hepatic differentiation proceeds, the morphology of hESCs gradually changed into a typical hepatocyte morphology, with distinct round nuclei and a polygonal shape (Fig. 2B), and the expression levels of hepatic markers

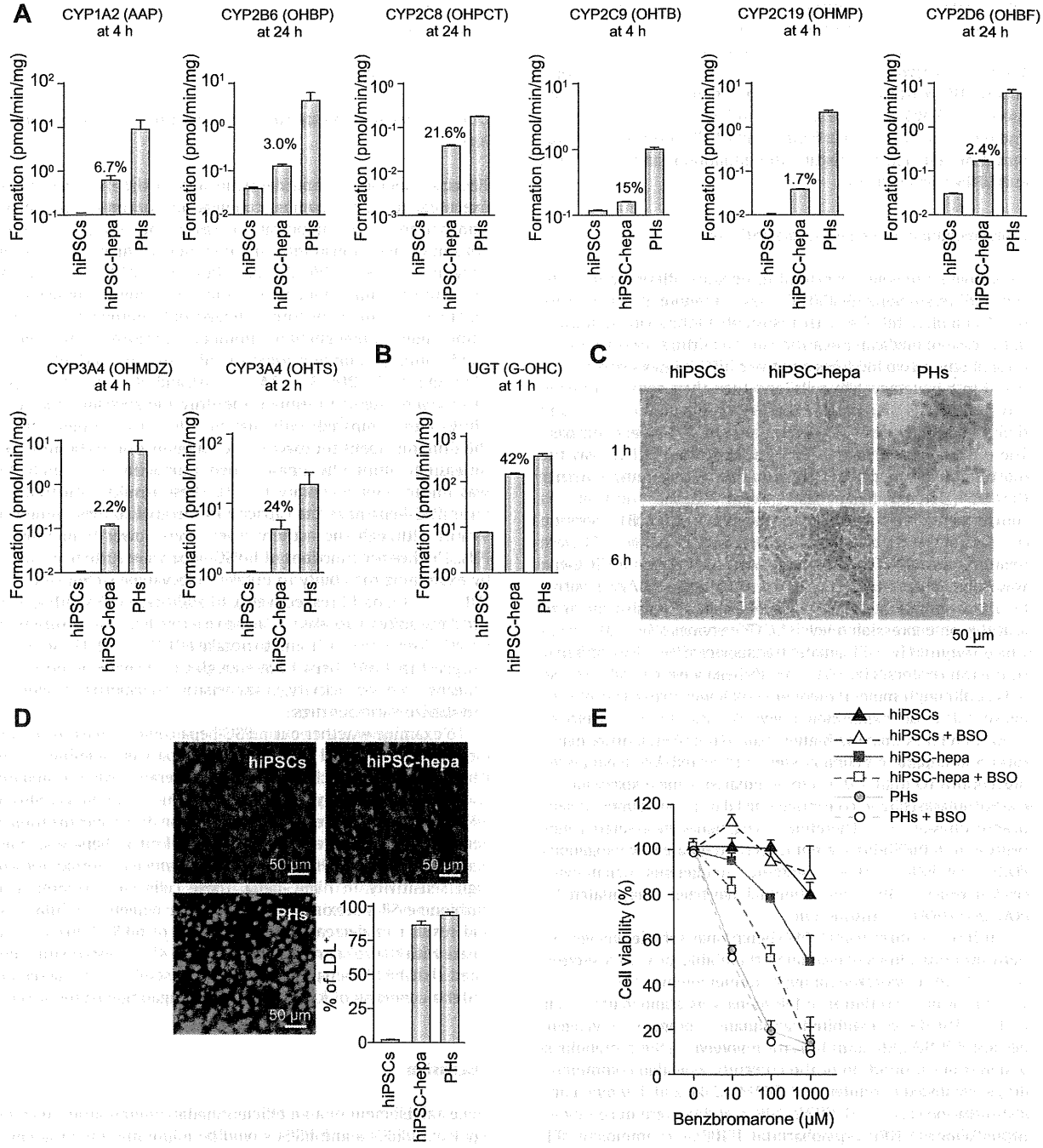

Fig. 4. Evaluation of the drug metabolism capacity and hepatic transporter activity of hiPSC-hepa. hiPSCs (Dotcom) were differentiated into hepatocytes as described in Fig. 2A. (A and B) Quantitation of metabolites in hiPSCs, hiPSC-hepa, and PHs, which were cultured for 48 h after the cells were plated, was examined by treating nine substrates (Phenacetin, Bupropion, Paclitazel, Tolbtamide, S-mephenytoin, Bufuralol, Midazolam, Testosterone, and Hydroxyl coumarin; these compounds are substrates for CYP1A2, 2B6, 2C8, 2C9, 2C19, 2D6, 3A4, 3A4 (A) and UGT (B), respectively), and then supernatants were collected at the indicated time. The quantity of metabolites (Acetaminophen [AAP], Hydroxybupropion [OHBP], 6α-hydroxypaclitaxel [OHPCT], Hydroxytolbutamide [OHTB], 4′-hydroxymephenytoin [OHMP], 1′-hydroxybufuralol [OHBF], 1′-hydroxymidazolam [OHMDZ], 6β-hydroxytestosterone [OHTS], 7-Hydroxycoumarin glucuronide [G-OHC], respectively) was measured by LC-MS/MS. The ratios of the activity levels in hiPSC-hepa to the activity levels in PHs rate are indicated in the graph. (C) hiPSCs, hiPSC-hepa, and PHs were examined for their ability to take up ICG (top) and release it 6 h thereafter (bottom). (D) hiPSCs, hiPSC-hepa, and PHs were cultured with medium containing Alexa-Flour 488-labeled LDL (green) for 1 h, and immunohistochemistry was performed. Nuclei were counterstained with DAPI (blue). The percentage of LDL-positive cells was also measured by FACS analysis. (E)

(ALB, CYP2D6, alpha-1-antitrypsin [αAT], CYP3A4, and CYP7A1) increased (Fig. 2C). Hepatic gene expression levels (Supplementary Fig. 6A), amount of ALB secretion (Supplementary Fig. 6B), and CYP2C9 activity level (Supplementary Fig. 6C) of Ad-FOXA2- and Ad-HNF1α-transduced cells were significantly higher than those of Ad-SOX17-, Ad-HEX-, and Ad-HNF4α-transduced cells. These results indicated that FOXA2 and HNF1α transduction promotes more efficiently hepatic differentiation than SOX17, HEX, and HNF4α transduction.

Characterization of the hESC-hepa/hiPSC-hepa

As we have previously reported [6], hepatic differentiation efficiency differs among hESC/hiPSC lines. Therefore, it is necessary to select a hESC/hiPSC line that is suitable for hepatic maturation in the case of medical applications such as drug screening. In the present study, two hESC lines and five hiPSCs lines were differentiated into hepatocyte-like cells, and then their gene expression levels of *ALB* (Fig. 3A) and *CYP3A4* (Supplementary Fig. 7A), and their CYP3A4 activities (Supplementary Fig. 7B) were compared. These data suggest that the iPSC line, Dotcom [11,12], was the most suitable for hepatocyte maturation. To examine whether the iPSC (Dotcom)-hepa has enough hepatic functions as compared with PHs, the amount of albumin (ALB) secretion (Fig. 3B) and the percentage of ALB-positive cells (Fig. 3C) were measured on day 20. The amount of ALB secretion in hiPSC-hepa was similar to that in PHs and the percentage of ALB-positive cells was approximately 90% in iPSC-hepa. We also confirmed that the gene expression levels of CYP enzymes (Fig. 3D), conjugating enzymes (Fig. 3E), hepatic transporters (Fig. 3F), and hepatic nuclear receptors (Fig. 3G) in hiPSC-hepa were similar to those of PHs, although some of them were still lower than those of PHs. Because the gene expression level of the fetal CYP isoform, *CYP3A7*, in hiPSC-hepa was higher than that of PHs, mature hepatocytes and hepatic precursors were still mixed. We have previously confirmed that Ad vector-mediated gene expression in the hepatoblasts (day 9) continued until day 14 and almost disappeared on day 18 [7]. Therefore, the hepatocyte-related genes expressed in hiPSC-hepa are not directly regulated by exogenous FOXA2 or HNF1α. Taken together, endogenous hepatocyte-related genes in hiPSC-hepa should have been upregulated by FOXA2 and HNF1α transduction.

To further confirm that hiPSC-hepa have sufficient levels of hepatocyte functions, we evaluated the ability of urea secretion (Fig. 3H) and glycogen storage (Supplementary Fig. 8). The amount of urea secretion in hiPSC-hepa was about half of that in PHs. HiPSC-hepa exhibited abundant storage of glycogen. Because CYP1A2, 2B6, and 3A4 are involved in the metabolism of a significant proportion of the currently available commercial drugs, we tested the induction of *CYP1A2*, *2B6*, and *3A4* by chemical stimulation (Fig. 3I). *CYP1A2*, *2B6*, and *3A4* are induced by β-naphthoflavone [bNF], phenobarbital [PB], or rifampicin [RIF], respectively. Although undifferentiated hiPSCs did not respond to either bNF, PB, or RIF (data not shown), hiPSC-hepa produced more metabolites in response to chemical stimulation, suggesting that inducible CYP enzymes were detectable in hiPSC-hepa (Fig. 3I). However, the induction potency of *CYP1A2*, *2B6*, and *3A4* in hiPSC-hepa were lower than that in PHs.

Drug metabolism capacity and hepatic transporter activity of hiPSC-hepa

Because metabolism and detoxification in the liver are mainly executed by CYP enzymes, conjugating enzymes, and hepatic transporters, it is important to assess the function of these enzymes and transporters in hiPSC-hepa. Among the various enzymes in liver, CYP1A2, 2B6, 2C8, 2C9, 2C19, 2D6 and 3A4, UGT are the important phase I and II enzymes responsible for metabolism. Nine substrates, Phenacetin, Bupropion, Paclitazel, Tolbtamide, *S*-mephenytoin, Bufuralol, Midazolam, Testosterone, and Hydroxyl coumarin, which are the substrates of CYP1A2, 2B6, 2C8, 2C9, 2C19, 2D6, 3A4, 3A4 (Fig. 4A), and UGT (Fig. 4B), respectively, were used to estimate the drug metabolism capacity of hiPSC-hepa compared with that of PHs. To precisely estimate the drug metabolism capacity, the amounts of metabolites were measured during the phase when production of metabolites was linear (Supplementary Fig. 9). These results indicated that our hiPSC-hepa have the capacity to metabolize these nine substrates, although the activity levels were lower than those of PHs. The hepatic functions of hiPSC-hepa were further evaluated by examining the ability to uptake Indocyanine Green (ICG) and LDL (Fig. 4C and D, respectively). In addition to PHs, hiPSC-hepa had the ability to uptake ICG and to excrete ICG in a culture without ICG for 6 h (Fig. 4C), and to uptake LDL (Fig. 4D). These results suggest that hiPSC-hepa have enough CYP enzyme activity, conjugating enzyme activity, and hepatic transporter activity to metabolize various drugs.

To examine whether our hiPSC-hepa could be used to predict metabolism-mediated toxicity, hiPSC-hepa were incubated with Benzbromarone, which is known to generate toxic metabolites, and then cell viability was measured (Fig. 4E). Cell viability of hiPSC-hepa was decreased depending on the concentration of Benzbromarone. However, cell viability of hiPSC-hepa was much higher than that of PHs. To detect drug–induced cytotoxicity with high sensitivity in hiPSC-hepa, these cells were treated with Buthionine-SR-sulfoximine (BSO), which depletes cellular GST, and result in a decrease of cell viability of hiPSC-hepa as compared with that of non-treated cells (Fig. 4E). These results indicated that hiPSC-hepa would be more useful in drug screening under a condition of knockdown of conjugating enzyme activity.

Discussion

The establishment of an efficient hepatic differentiation technology from hESCs and hiPSCs would be important for the application of hESC-hepa and hiPSC-hepa to drug toxicity screening. Although we have previously reported that sequential transduc-

The cell viability of hiPSCs, hiPSC-hepa, PHs, and their BSO-treated cells (0.4 mM BSO was pre-treated for 24 h) was assessed by Alamar Blue assay after 48-hr exposure to differe2nt concentrations of benzbromarone. The cell viability is expressed as a percentage of that in cells treated only with solvent. All data are represented as mean ± SD (n = 3).

tion of SOX17, HEX, and HNF4α into hESC-derived cells could promote efficient hepatic differentiation [7], further hepatic maturation of the hESC-hepa and hiPSC-hepa was needed for this application. To further improve the differentiation efficiency of every step of hepatic differentiation (hESC to DE cells, DE cells to hepatoblasts, and hepatoblasts to hESC-hepa), we initially performed a screening of transcription factors. In the stage of DE differentiation, FOXA2 transduction could promote the most efficient DE differentiation (Fig. 1C). In the stage of hepatic commitment, expansion, and maturation, the combination of FOXA2 and HNF1α transduction strongly promoted hepatic commitment and maturation (Fig. 1F and J), although in the stage of hepatic expansion and maturation, HNF4α transduction was as efficient as that of HNF1α (Fig. 1J). Since HNF1α is one of the target genes of HNF4α [13], the signaling through HNF4α to HNF1α would be important for efficient hepatic expansion and maturation. Considering these results together, we ascertained a pair of two transcription factors, FOXA2 and HNF1α, that could promote efficient hepatic differentiation from hESCs. In embryogenesis, the expression of FOXA2 and HNF1α is initially detected in DE or hepatoblasts, respectively and the expression levels of both FOXA2 and HNF1α are elevated as the liver develops [14,15]. Therefore, our hepatic differentiation technology, which employs FOXA2 and HNF1α transduction, might mimic the gene expression pattern during embryogenesis.

We found that the gene expression levels of CYP enzymes, conjugating enzymes, hepatic transporters, and hepatic nuclear receptors were upregulated by FOXA2 and HNF1α transduction (Fig. 3D–G). In contrast to the high expression levels of hepatocyte-related genes, CYP induction potency and the drug metabolism capacity of our hiPSC-hepa were lower than those of PHs (Figs. 3I and 4A and B). One of the possible reasons for the difference between gene expression levels of CYP enzymes and CYP induction activity might be that there were insufficient expression levels of hepatic nuclear receptors (such as *PXR*, *SHR*, and *FXR*) in hiPSC-hepa (Fig. 3G). Because many CYPs require high expression levels of hepatic nuclear receptor for efficient drug metabolism [16], transduction of these hepatic nuclear receptor genes in hiPSC-hepa or development of a differentiation method that induces high expression of these nuclear receptors might improve the drug metabolic capacity. Another explanation for the low CYP activities in hiPSC-hepa, maybe that hiPSCs were established from an individual with low CYP activities; infact, it is known that large individual differences in CYP activities are observed among individuals. It might be important to use a hiPSC line established from a person with high CYP activities. It is essential to investigate the reasons behind this significant discordance, an issue that our group is currently planning to study.

In summary, our method, consisting of sequential FOXA2 and HNF1α transduction along with the addition of adequate soluble factors at each step of differentiation, is a valuable tool for the efficient generation of functional hepatocytes derived from hESCs and hiPSCs. The hiPSC-hepa exhibited a number of hepatocyte functions (such as ALB secretion, uptake of LDL or ICG, glycogen storage, and drug metabolism capacity). In addition, the hiPSC-hepa were successfully applied to the evaluation of drug-induced cytotoxicity. Therefore, the hESC-hepa and hiPSC-hepa might be used for drug screening in early phases of pharmaceutical development.

Conflict of interest

The authors who have taken part in this study declared that they do not have anything to disclose regarding funding or conflict of interest with respect to this manuscript.

Acknowledgements

We thank Misae Nishijima, Nobue Hirata, Miki Yoshioka, and Hiroko Matsumura for their excellent technical support. We thank Ms. Ong Tyng Tyng for critical reading of the manuscript. HM, MKF, and TH were supported by grants from the Ministry of Health, Labor, and Welfare of Japan. HM was also supported by Japan Research foundation For Clinical Pharmacology, The Nakatomi Foundation, and The Uehara Memorial Foundation. K. Kawabata was supported by Grants from the Ministry of Education, Sports, Science and Technology of Japan (20200076) and the Ministry of Health, Labor, and Welfare of Japan. K. Katayama and FS were supported by Program for Promotion of Fundamental Studies in Health Sciences of the National Institute of Biomedical Innovation (NIBIO).

Supplementary data

Supplementary data associated with this article can be found, in the online version, at http://dx.doi.org/10.1016/j.jhep.2012.04.038.

References

[1] Thomson JA, Itskovitz-Eldor J, Shapiro SS, Waknitz MA, Swiergiel JJ, Marshall VS, et al. Embryonic stem cell lines derived from human blastocysts. Science 1998;282:1145–1147.
[2] Takahashi K, Tanabe K, Ohnuki M, Narita M, Ichisaka T, Tomoda K, et al. Induction of pluripotent stem cells from adult human fibroblasts by defined factors. Cell 2007;131:861–872.
[3] Clayton DF, Darnell Jr JE. Changes in liver-specific compared to common gene transcription during primary culture of mouse hepatocytes. Mol Cell Biol 1983;3:1552–1561.
[4] Snykers S, De Kock J, Rogiers V, Vanhaecke T. In vitro differentiation of embryonic and adult stem cells into hepatocytes: state of the art. Stem cells 2009;27:577–605.
[5] Inamura M, Kawabata K, Takayama K, Tashiro K, Sakurai F, Katayama K, et al. Efficient generation of hepatoblasts from human ES cells and iPS cells by transient overexpression of homeobox gene HEX. Mol Ther 2011;19:400–407.
[6] Takayama K, Inamura M, Kawabata K, Tashiro K, Katayama K, Sakurai F, et al. Efficient and directive generation of two distinct endoderm lineages from human ESCs and iPSCs by differentiation stage-specific SOX17 transduction. PLoS One 2011;6:e21780.
[7] Takayama K, Inamura M, Kawabata K, Katayama K, Higuchi M, Tashiro K, et al. efficient generation of functional hepatocytes from human embryonic stem cells and induced pluripotent stem cells by HNF4alpha transduction. Mol Ther 2012;20:127–137.
[8] Duan Y, Ma X, Zou W, Wang C, Bahbahan IS, Ahuja TP, et al. Differentiation and characterization of metabolically functioning hepatocytes from human embryonic stem cells. Stem cells 2010;28:674–686.
[9] Furue MK, Na J, Jackson JP, Okamoto T, Jones M, Baker D, et al. Heparin promotes the growth of human embryonic stem cells in a defined serum-free medium. Proc Natl Acad Sci U S A 2008;105:13409–13414.
[10] Lacroix D, Sonnier M, Moncion A, Cheron G, Cresteil T. Expression of CYP3A in the human liver–evidence that the shift between CYP3A7 and CYP3A4 occurs immediately after birth. Eur J Biochem 1997;247:625–634.

[11] Nagata S, Toyoda M, Yamaguchi S, Hirano K, Makino H, Nishino K, et al. Efficient reprogramming of human and mouse primary extra-embryonic cells to pluripotent stem cells. Genes Cells 2009;14:1395–1404.
[12] Makino H, Toyoda M, Matsumoto K, Saito H, Nishino K, Fukawatase Y, et al. Mesenchymal to embryonic incomplete transition of human cells by chimeric OCT4/3 (POU5F1) with physiological co-activator EWS. Exp Cell Res 2009;315:2727–2740.
[13] Gragnoli C, Lindner T, Cockburn BN, Kaisaki PJ, Gragnoli F, Marozzi G, et al. Maturity-onset diabetes of the young due to a mutation in the hepatocyte nuclear factor-4 alpha binding site in the promoter of the hepatocyte nuclear factor-1 alpha gene. Diabetes 1997;46:1648–1651.
[14] Ang SL, Wierda A, Wong D, Stevens KA, Cascio S, Rossant J, et al. The formation and maintenance of the definitive endoderm lineage in the mouse: involvement of HNF3/forkhead proteins. Development 1993;119: 1301–1315.
[15] Kyrmizi I, Hatzis P, Katrakili N, Tronche F, Gonzalez FJ, Talianidis I. Plasticity and expanding complexity of the hepatic transcription factor network during liver development. Genes Dev 2006;20:2293–2305.
[16] Lehmann JM, McKee DD, Watson MA, Willson TM, Moore JT, Kliewer SA. The human orphan nuclear receptor PXR is activated by compounds that regulate CYP3A4 gene expression and cause drug interactions. J Clin Invest 1998;102:1016–1023.

Biomaterials 33 (2012) 4526–4534

Contents lists available at SciVerse ScienceDirect

Biomaterials

journal homepage: www.elsevier.com/locate/biomaterials

The promotion of hepatic maturation of human pluripotent stem cells in 3D co-culture using type I collagen and Swiss 3T3 cell sheets

Yasuhito Nagamoto [a,b], Katsuhisa Tashiro [b], Kazuo Takayama [a,b], Kazuo Ohashi [d], Kenji Kawabata [b,c], Fuminori Sakurai [a], Masashi Tachibana [a], Takao Hayakawa [e,f], Miho Kusuda Furue [g,h], Hiroyuki Mizuguchi [a,b,i,*]

[a] Laboratory of Biochemistry and Molecular Biology, Graduate School of Pharmaceutical Sciences, Osaka University, Osaka 565-0871, Japan
[b] Laboratory of Stem Cell Regulation, National Institute of Biomedical Innovation, Osaka 567-0085, Japan
[c] Laboratory of Biomedical Innovation, Graduate School of Pharmaceutical Sciences, Osaka University, Osaka 565-0871, Japan
[d] Institute of Advanced Biomedical Engineering and Science, Tokyo Women's Medical University, Tokyo 162-8666, Japan
[e] Pharmaceutics and Medical Devices Agency, Tokyo 100-0013, Japan
[f] Pharmaceutical Research and Technology Institute, Kinki University, Osaka 577-8502, Japan
[g] Laboratory of Cell Cultures, Department of Disease Bioresources, National Institute of Biomedical Innovation, Osaka 567-0085, Japan
[h] Laboratory of Cell Processing, Institute for Frontier Medical Sciences, Kyoto University, Kyoto 606-8507, Japan
[i] The Center for Advanced Medical Engineering and Informatics, Osaka University, Osaka 565-0871, Japan

ARTICLE INFO

Article history:
Received 16 February 2012
Accepted 3 March 2012
Available online 23 March 2012

Keywords:
Hepatocyte
Co-culture
Collagen
Fibroblast
Liver
ECM (extracellular matrix)

ABSTRACT

Hepatocyte-like cells differentiated from human embryonic stem cells (hESCs) or human induced pluripotent stem cells (hiPSCs) are known to be a useful cell source for drug screening. We recently developed an efficient hepatic differentiation method from hESCs and hiPSCs by sequential transduction of FOXA2 and HNF1α. It is known that the combination of three-dimensional (3D) culture and co-culture, namely 3D co-culture, can maintain the functions of primary hepatocytes. However, hepatic maturation of hESC- or hiPSC-derived hepatocyte-like cells (hEHs or hiPHs, respectively) by 3D co-culture systems has not been examined. Therefore, we utilized a cell sheet engineering technology to promote hepatic maturation. The gene expression levels of hepatocyte-related markers (such as cytochrome P450 enzymes and conjugating enzymes) and the amount of albumin secretion in the hEHs or hiPHs, which were 3D co-cultured with the Swiss 3T3 cell sheet, were significantly up-regulated in comparison with those in the hEHs or hiPHs cultured in a monolayer. Furthermore, we found that type I collagen synthesized in Swiss 3T3 cells plays an important role in hepatic maturation. The hEHs or hiPHs that were 3D co-cultured with the Swiss 3T3 cell sheet would be powerful tools for medical applications, such as drug screening.

1. Introduction

Several studies have recently shown the ability of human embryonic stem cells (hESCs) [1] and human induced pluripotent stem cells (hiPSCs) [2] to differentiate into hepatocyte-like cells [3–6]. Although primary human hepatocytes are generally employed for drug toxicity screening in the early phase of pharmaceutical development, these cells have some drawbacks, such as their limited range of sources, difference in variability and functions from batch to batch, and de-differentiation. Because hESC- or hiPSC-derived hepatocyte-like cells (hEHs or hiPHs, respectively) have potential to resolve these problems, they are expected to be applied to drug screening. The hepatic differentiation processes from hESCs and hiPSCs are divided into three-stages, differentiation into definitive endoderm (DE) cells, hepatoblasts, and mature hepatocytes. Hepatic differentiation methods based on the treatment of growth factors have been widely used to generate hepatocyte-like cells from hESCs or hiPSCs [5–9]. However, the hepatic differentiation efficiency is not high enough for medical applications such as drug screening [10]. To promote the efficiency of hepatic differentiation and hepatic maturation, we have developed hepatic differentiation methods that combine the transduction of transcription factor genes involved in liver development

* Corresponding author. Laboratory of Biochemistry and Molecular Biology, Graduate School of Pharmaceutical Sciences, Osaka University, 1-6 Yamadaoka, Suita, Osaka 565-0871, Japan. Tel.: +81 6 6879 8185; fax: +81 6 6879 8186.
E-mail address: mizuguch@phs.osaka-u.ac.jp (H. Mizuguchi).

0142-9612/$ – see front matter © 2012 Elsevier Ltd. All rights reserved.
doi:10.1016/j.biomaterials.2012.03.011

with stimulation by growth factors [11–13]. The hepatocyte-like cells generated by our protocols have levels of expression of hepatocyte-related genes similar to the levels in (cryopreserved) primary human hepatocytes cultured for 48 h after plating [12]. Moreover, we have recently established more efficient and simple methods for hepatic differentiation from hESCs and hiPSCs by sequential transduction of forkhead box A2 (FOXA2) and hepatocyte nuclear factor 1 homeobox A (HNF1α) (in submitted). In that recent study, we showed that the hEHs or hiPHs expressed the genes of hepatocyte-related markers at levels similar to those in primary human hepatocytes and could metabolize various types of drugs.

It is known that cell–cell interactions between hepatocytes and their surrounding cells are essential for liver development and maintenance of liver functions [14–17]. Although primary human hepatocytes rapidly lose their functions under a monolayer culture condition, they could retain their functions, such as albumin secretion and urea synthesis, in three-dimensional (3D) culture and co-culture [18–21]. Moreover, it has been reported that the primary hepatocytes maintain their functions for a long time by the combination of 3D culture and co-culture, namely 3D co-culture [22–24]. In particular, the functions of primary rat hepatocytes cultured in a 3D co-culture, were shown to be more efficiently preserved than the functions of primary rat hepatocytes cultured in monolayer a co-culture [24]. Recently, Kim et al. reported that primary rat hepatocytes are able to maintain their functions in 3D co-culture with an endothelial cell sheet [25]. To perform 3D co-culture with a cell sheet, they employed cell sheet engineering technology using temperature-responsive culture dishes grafted with a temperature-responsive polymer, poly(*N*-isopropylacrylamide). This cell sheet engineering technology make it possible to manipulate a monolayer cell sheet with the extracellular matrices (ECMs) synthesized from the cells [26]. Although 3D culture or co-culture methods have been individually applied to promote hepatic differentiation from ESCs or iPSCs [27–29], few studies have investigated the hepatic differentiation from hESCS or hiPSCs using a 3D co-culture method.

In this study, we examined whether 3D co-culture, which uses the cell sheet engineering technology, could promote hepatic differentiation, and particularly the differentiation into mature hepatocyte-like cells, from hESCs and hiPSCs. Because Swiss 3T3 cells are widely used for co-culture with primary hepatocytes [18–20], we employed Swiss 3T3 cells for 3D co-culture with the hEHs or hiPHs. After hEHs and hiPHs were 3D co-cultured with a Swiss 3T3 cell sheet, we examined the expression levels of hepatocyte-related genes. Moreover, we investigated a Swiss 3T3 cell-derived factor that can promote hepatic maturation from hESCs and hiPSCs.

2. Materials and methods

2.1. hESC and hiPSC culture

A hESC line, H9 (WiCell Research Institute), was maintained on a feeder layer of mitomycin C (MMC)-treated mouse embryonic fibroblasts (MEF, Millipore) with ReproStem (ReproCELL) supplemented with 5 ng/ml fibroblast growth factor 2 (FGF2) (Sigma). hESCs were dissociated with 0.1 mg/ml dispase (Roche Diagnostics) into small clumps and were then subcultured every 4 or 5 days. H9 cells were was used following the Guidelines for Derivation and Utilization of Human Embryonic Stem Cells of the Ministry of Education, Culture, Sports, Science and Technology of Japan. One hiPSC line generated from the human embryonic lung fibroblast cell line MCR5 was provided from the JCRB Cell Bank (Tic, JCRB Number: JCRB1331). Another hiPSC line, 201B7, generated from human dermal fibroblasts was kindly provided by Dr. S. Yamanaka (KyotoUniversity). These hiPSC lines were maintained on a feeder layer of MMC-treated MEF with iPSellon (for Tic, Cardio) or ReproStem (for 201B7, ReproCELL) supplemented with 10 ng/ml (for Tic) or 5 ng/ml (for 201B7) FGF2.hiPSCs were dissociated with 0.1 mg/ml dispase (Roche Diagnostics) into small clumps and were then subcultured every 5 or 6 days.

2.2. Swiss 3T3 cell culture

A mouse fibroblast line, Swiss 3T3, was maintained with RPMI-1640 medium (Sigma) supplemented with fetal bovine serum (10%) (FBS), streptomycin (120 μg/ml), and penicillin (200 μg/ml).

2.3. Ad vectors

The human eukaryotic translation elongation factor 1 alpha 1 (EF-1α) promoter-driven HNF1α- and FOXA2-expressing Ad vectors (Ad-HNF1α and Ad-FOXA2, respectively) were constructed previously (in submitted). All of Ad vectors contain a stretch of lysine residue (K7) peptides in the C-terminal region of the fiber knob for more efficient transduction of hESCs, hiPSCs, and DE cells, in which transduction efficiency was almost 100%, and purified as described previously [11,12,30]. The vector particle (VP) titer was determined by using a spectrophotometric method [31].

2.4. In vitro differentiation

Before the initiation of cellular differentiation, the medium of hESCs and hiPSCs was exchanged for a defined serum-free medium, hESF9, and hESCs and hiPSCs were cultured as previously reported [32]. The differentiation protocol for the induction of DE cells, hepatoblasts, and hepatocytes was based on our previous report with some modifications (in submitted). Briefly, in mesendoderm differentiation, hESCs and hiPSCs were dissociated into single cells by using Accutase (Millipore) and cultured for 2 days on Matrigel (BD Biosciences) in hESF-DIF medium (Cell Science & Technology Institute) supplemented with 10 μg/ml human recombinant insulin, 5 μg/ml human apotransferrin, 10 μM 2-mercaptoethanol, 10 μM ethanolamine, 10 μM sodium selenite, and 0.5 mg/ml bovine serum albumin (BSA) (all from Sigma) (differentiation hESF-DIF medium) containing 100 ng/ml Activin A (R&D Systems) and 10 ng/ml FGF2. To generate DE cells, hESC- or hiPSC-derived mesendoderm cells were transduced with 3000 VP/cell of Ad-FOXA2 for 1.5 h on day 2 and cultured until day 6 on Matrigel in differentiation hESF-DIF medium supplemented with 100 ng/ml Activin A and 10 ng/ml FGF2. For induction of the hepatoblasts, the hESC- or hiPSC-derived DE cells were transduced with each 1500 VP/cell of Ad-FOXA2 and Ad-HNF1α for 1.5 h on day 6 and cultured for 3 days on Matrigel in hepatocyte culture medium (HCM) (Lonza) supplemented with 30 ng/ml bone morphogenetic protein 4 (BMP4) and 20 ng/ml FGF4 (all from R&D Systems). To expand the hepatoblasts, the hepatoblasts were transduced with each 1500 VP/cell of Ad-FOXA2 and Ad-HNF1α for 1.5 h on day 9 and cultured for 3 days on Matrigel in HCM supplemented with 10 ng/ml hepatocyte growth factor (HGF), 10 ng/ml FGF1, 10 ng/ml FGF4, and 10 ng/ml FGF10 (all from R&D Systems).To induce hepatic maturation, the cells were cultured for 2 days on Matrigel in L15 medium (Invitrogen) supplemented with 8.3% tryptose phosphate broth (BD Biosciences), 10% FBS (Vita), 10 μM hydrocortisone 21-hemisuccinate (Sigma), 1 μM insulin, and 25 mM NaHCO3 (Wako) (differentiation L15 medium) containing 20 ng/ml hepatocyte growth factor (HGF), 20 ng/ml Oncostatin M (OsM) (R&D Systems), and 10^{-6} M Dexamethasone (DEX) (Sigma). As described below, the Swiss 3T3 cell sheet was stratified onto hepatocyte-like cells on day 14 and cultured in differentiation L15 medium supplemented with 20 ng/ml HGF, 20 ng/ml OsM, and 10^{-6} M DEX until day 15. On day 15, Matrigel was stratified onto the cells and cultured in differentiation L15 medium supplemented with 20 ng/ml HGF, 20 ng/ml OsM, and 10^{-6} M DEX until day 25.

2.5. Cell sheet harvesting and stratifying procedure utilizing a gelatin-coated manipulator

The stratifying protocol was performed as previously described with some modifications [25,33]. Briefly, Swiss 3T3 cells were seeded on a 24-well temperature-responsive culture plate (TRCP) (Cell Seed Inc, Tokyo) on day 12. Two days after seeding (day 14), Swiss 3T3 cells were grown to confluence. On the same day (day 14), a gelatin-coated cell sheet manipulator was placed on the Swiss 3T3 cells, and the culture temperature was reduced to 20 °C for 60 min. By removing the manipulator, cultured Swiss 3T3 cells were harvested as a contiguous cell sheet that attached on the gelatin. The Swiss 3T3 cell sheet was then stratified on the hEHs or hiPHs. The culture plate with the manipulator was incubated at room temperature for 60 min to induce adherence between the hEHs or hiPHs and Swiss 3T3 cell sheet. To dissolve the gelatin, the culture plate was incubated at 37 °C for 60 min, and this was followed by several washing steps.

2.6. RNA isolation and reverse transcription-PCR

Total RNA was isolated from the hESC- or hiPSC-derived cells using ISOGENE (Nippon Gene) according to the manufacturer's instructions. cDNA was synthesized using 500 ng of total RNA with a Superscript VILO cDNA synthesis kit (Invitrogen). Real-time RT-PCR was performed with Taqman gene expression assays or Fast SYBR Green Master Mix using an ABI Step One Plus (all from Applied Biosystems). Relative quantification was performed against a standard curve and the values were normalized against the input determined for the housekeeping gene, *glyceraldehyde 3-phosphate dehydrogenase* (*GAPDH*). The primer sequences used in this study are described in Supplementary Tables 1 and 2.

2.7. Preparation of verticalsection

On day 15, the hEHs cultured with or without the Swiss 3T3 cell sheet were frozen in Tissue-Tek O.C.T. Compound (Sakura Finetek), then vertically sectioned and fixed with 4% paraformaldehyde. These sections were monitored by a phase contrast microscope (Olympus).

2.8. ELISA

hESCs or hiPSCs were differentiated into the hepatocyte-like cells as described in Fig. 1A. The culture supernatants, which were incubated for 24 h after fresh medium was added, were collected and analyzed to determine the amount of ALB secretion by ELISA. ELISA kits for ALB were purchased from Bethyl Laboratories. ELISA was performed according to the manufacturer's instructions. The amount of ALB secretion was calculated according to each standard.

2.9. Co-culture and culture in a cell culture insert system (insert-culture)

hESCs were differentiated into the hepatocyte-like cells as described in Fig. 1A until day 14, and then the hESC-derived cells were harvested and seeded onto a 6-well culture plate (Falcon) with Swiss 3T3 (1:1) in a co-culture system. In a insert-culture system, hESC-derived hepatocyte-like cells were harvested and seeded onto a 6-well culture plate alone, and Swiss 3T3 cells were plated in cell culture inserts (membrane pore size 1.0 μm; Falcon), and placed in a well of the culture palate containing hESC-derived hepatocyte-like cells. These cells were cultured in differentiation L15 medium supplemented with 20 ng/ml HGF, 20 ng/ml OsM, and 10^{-6} M DEX until day 25.

2.10. Stratification of type I collagen gel

A type I collagen gel solution was prepared as suggested by Nitta Gelatin: 7 parts of solubilized collagen in HC1 (pH 3.0) 2 parts of 5× concentrated RPMI-1640 medium, and 2 parts of reconstitution buffer (0.2 M HEPES, 0.08 M NaOH) to neutralize the collagen gel, were mixed gently but rapidly at 4 °C. Next, the hESC-derived cells were cultured in a type I collagen gel solution for 3h, and then the medium waschanged and the cells were cultured in differentiation L15 medium supplemented with 20 ng/ml HGF, 20 ng/ml OsM, and 10^{-6} M DEX until day 25.

2.11. Inhibition of collagen synthesis

hESCs were differentiated into the hepatocyte-like cells as described in Fig. 1A until stratification of the Swiss 3T3 cell sheet. After stratification of the Swiss 3T3 cell sheet, the cells were cultured in differentiation L15 medium supplemented with 20 ng/ml HGF, 20 ng/ml OsM, 10^{-6} M DEX, and 25 μM 2,2′-Bipyridyl (Wako), an inhibitor of collagen synthesis, until day 25.

2.12. Western blotting analysis

Swiss 3T3 cells were cultured with 25 μM 2,2′-Bipyridyl or solvent (0.1% DMSO) for 3 days, and these cells were then homogenized with lysis buffer (1% Nonidet P-40, 1 mM EDTA, 25 mM Tris-HCl, 5 mM NaF, and 150 mM NaCl) containing protease inhibitor mixture (Sigma-Aldrich). After being frozen and thawed, the homogenates were centrifuged at 15,000× *g* at 4 °C for 10 min, and the supernatants were collected. The lysates were subjected to SDS-PAGE on 7.5% polyacrylamide gel and were then transferred onto polyvinylidene fluoride membranes (Millipore). After the reaction was blocked with 1% skim milk in TBS containing 0.1% Tween 20 at room temperature for 1 h, the membranes were incubated with goat anti-col1a1 Ab (diluted 1/200; Santa Cruz Biotechnology) or mouse anti-β-actin Ab (diluted 1/5000; Sigma) at 4 °C overnight, followed by reaction with horseradish peroxidase-conjugated anti-goat IgG (Chemicon) or anti-mouse IgG (Cell Signaling Technology) at room temperature for 1 h. The band was visualized by ECL Plus Western blotting detection reagents (GE Healthcare) and the signals were read using a LAS-3000 imaging system (FUJI Film).

2.13. Statistical analysis

Statistical analysis was performed using the unpaired two-tailed Student's *t*-test.

3. Results

3.1. Efficient hepatic maturation by stratification of the Swiss 3T3 cell sheet

The hEHs, which were generated by the transduction of *HNF1α* and *FOXA2* genes, were 3D co-cultured with the Swiss 3T3 cell sheet to promote hepatic differentiation and to generate mature hepatocytes from hESCs and hiPSCs. Our differentiation strategy using the stratification of the Swiss 3T3 cell sheet is illustrated in Fig. 1A. The stratifying procedure was performed on day 14 as described in Fig. 1B. The day after stratifying the Swiss 3T3 cell sheet on the hEHs, vertical sections of the monolayer hEHs (hEHs-mono) and the hEHs stratified with the Swiss 3T3 cell sheet (hEHs-Swiss) were prepared (Fig. 1C). We found that Swiss 3T3 cells were successfully harvested and overlaid onto the hEHs as a monolayer cell sheet (Fig. 1C). Moreover, the hEHs seemed to be larger than the Swiss 3T3 cells. The space between the hEHs cells and Swiss 3T3 cells suggests the formation of ECMs (Fig. 1C).

To investigate whether stratification of the Swiss 3T3 cell sheet could promote hepatic maturation of the hEHs, hESCs (H9) were differentiated into the hepatocyte-like cells according to the protocol described in Fig. 1A, and then the gene expression levels of hepatocyte-related markers and the amount of albumin (ALB) secretion in the hEHs-Swiss were measured on day 25 (Fig. 2). By 3D co-culturing of the hepatocyte-like cells with the Swiss 3T3 cell sheet for 10 days (days 15–25), the gene expression levels of hepatocyte-related markers, such as *ALB* (Fig. 2A), *hepatocyte nuclear factor 4 alpha* (*HNF4A*) (Fig. 2B), cytochrome P450 (CYP) enzymes (*CYP2C9*, *CYP7A1*, *CYP1A2*, and *CYP3A5*) (Fig. 2D–G), and conjugating enzymes (*glutathione S-transferase alpha 1* [*GSTA1*], *GSTA2*, and *UDP glucuronosyltransferase* [*UGT1A1*]) (Fig. 2H–J) were significantly increased as compared with those in hEHs-mono. Moreover, the amount of ALB secretion in hEHs-Swiss was also up-regulated as compared with that in hEHs-mono (Fig. 2K). Because it is known that hepatoblasts can differentiate into hepatocytes and cholangiocytes [34,35], we examined the gene expression level of *cytokeratin 7* (*CK7*), a cholangiocyte-related marker, in hEHs-Swiss and hEHs-mono. In 3D co-culture with the Swiss 3T3 cell sheet, the gene expression level of *CK7* was down-regulated in the hEHs-Swiss relative to the hEHs-mono (Fig. 2C). These results clearly showed that stratification of the Swiss 3T3 cell sheet could promote the hepatic maturation of the hEHs and, in turn, suppress the cholangiocyte differentiation.

In order to investigate whether stratification of the Swiss 3T3 cell sheet promotes maturation of hiPHs as well as hEHs, the hiPSCs (Tic and 201B7) were differentiated into the hepatocyte-like cells according to the protocol described in Fig. 1A. The results showed that the gene expression levels of *ALB*, *CYP2C9*, *CYP3A5*, *CYP1A2*, and *GSTA1* in the hiPHs stratified with the Swiss 3T3 cell sheet (hiPHs-Swiss) were up-regulated in comparison with those in the monolayer hiPHs (hiPHs-mono) (Fig. 3A–E). Moreover, the gene expression level of *CK7* was markedly decreased in hiPHs-Swiss (Fig. 3F). The gene expression level of *ALB* in the hiPHs-Swiss differentiated from Tic was higher than that in the hiPHs-Swiss differentiated from 201B7, while the gene expression levels of CYP enzymes in the hiPHs-Swiss differentiated from Tic were lower than those in the hiPHs-Swiss differentiated from 201B7 (Fig. 3A–D). These results showed that stratification of the Swiss 3T3 cell sheet promoted hepatic maturation of both hEHs and hiPHs.

3.2. Identification of maturation factors synthesized from Swiss 3T3 cells

The data described above indicate that hepatic maturation factors were produced in Swiss 3T3 cells. To elucidate the Swiss 3T3 cell-derived hepatic maturation factors, the hEHs were cultured in cell culture-insert systems (insert-cultured), in which the hEHs were co-cultured with Swiss 3T3 cells without physical contacts, or co-cultured with Swiss 3T3 cells. Quantitative PCR analysis revealed that the gene expression levels of *ALB* and *CYP2C9* in the insert-cultured hEHs were increased in comparison with the hEHs-mono, while the expression levels of these genes were lower than